

Characterizing Catchment-Scale Nitrogen Legacies and Constraining their Uncertainties

F. J. Sarrazin¹, R. Kumar¹, N. B. Basu^{2,3,4}, A. Musolf⁵, M. Weber¹, K. Van
Meter^{6,7}, S. Attinger^{1,8}

¹Department of Computational Hydrosystems, Helmholtz-Centre for Environmental Research - UFZ,
Leipzig, Germany

²Department of Civil and Environmental Engineering, University of Waterloo, Waterloo, ON, Canada

³Department of Earth and Environmental Sciences, University of Waterloo, Waterloo, ON, Canada

⁴Water Institute, University of Waterloo, Waterloo, ON, Canada

⁵Department of Hydrogeology, Helmholtz-Centre for Environmental Research - UFZ, Leipzig, Germany

⁶Department of Geography, Pennsylvania State University, PA, USA

⁷Earth and Environmental Systems Institute, Pennsylvania State University, PA, USA

⁸Institute of Environmental Science and Geography, University of Potsdam, Potsdam, Germany

Key Points:

- We use a parsimonious model to examine the long-term (1960–2015) fate of nitrogen inputs to the landscape including the legacy buildup
- More than 50% of the nitrogen surplus denitrifies and around 491 kg ha^{-1} accumulates in legacy stores in Germany's largest river basin
- Hydrologic travel time and denitrification rates largely contribute to the residual uncertainty in the simulated nitrogen legacies

Corresponding author: Fanny Sarrazin, fanny.sarrazin@ufz.de

Corresponding author: Rohini Kumar, rohini.kumar@ufz.de

Abstract

Improving nitrogen (N) status in European water bodies is a pressing issue. N levels depend not only on current but also past N inputs to the landscape, that have accumulated through time in legacy stores (e.g. soil, groundwater). Catchment-scale N models, that are commonly used to investigate in-stream N levels, rarely examine the magnitude and dynamics of legacy components. This study aims to gain a better understanding of the long-term fate of the N inputs and its uncertainties, using a legacy-driven N model (ELEM_ENT) in Germany's largest national river basin (Weser; 38,450 km²) over the period 1960–2015. We estimate the nine model parameters based on a progressive constraining strategy, to assess the value of different observational datasets. We demonstrate that beyond in-stream N loading, soil N content and in-stream N concentration allow to reduce the equifinality in model parameterizations. We find that more than 50% of the N surplus denitrifies (1480–2210 kg ha⁻¹) and the stream export amounts to around 18% (410–640 kg ha⁻¹), leaving behind as much as around 230–780 kg ha⁻¹ of N in the (soil) source zone and 10–105 kg ha⁻¹ in the subsurface. A sensitivity analysis reveals the importance of different factors affecting the residual uncertainties in simulated N legacies, namely hydrologic travel time, denitrification rates, a coefficient characterising the protection of organic N in source zone and N surplus input. Our study calls for proper consideration of uncertainties in N legacy characterization, and discusses possible avenues to further reduce the equifinality in water quality modelling.

Plain Language Summary

Lowering nitrogen (N) amounts in European surface waters is a pressing issue. N levels largely result from fertilizer application in agricultural areas, and deposition of atmospheric N coming from fossil fuel combustion. These N inputs to the landscape can accumulate below the ground surface in so-called legacy stores (including the soil and aquifer), from which they can be released progressively through time. Therefore, N levels depend not only on the recent N inputs, but also on their history. Our modelling study aims to improve our understanding of the long-term fate of the N inputs and its uncertainties in Germany's largest national river basin (Weser) over the period 1960–2015. It suggests that more than 50% of the N inputs to land is lost to the atmosphere (denitrification, 1480–2210 kg ha⁻¹) and the stream export amounts to around 18% (410–640 kg ha⁻¹), leaving behind as much as around 16% (264–820 kg ha⁻¹) in the landscape (legacy). However, the uncertainties in these estimates remain large, partly due to a lack of observational data on internal (legacy)

53 components and uncertainties in N inputs. Overall, our study calls for proper consideration
54 of uncertainties in N legacy characterization, and discusses possible avenues to further reduce
55 them.

56 **1 Introduction**

57 Since the beginning of the 20th century, nitrogen (N) inputs to soils have increased
58 tremendously worldwide, due to application of synthetic N fertilizers and manure in agricul-
59 tural areas (Lu & Tian, 2017; B. Zhang et al., 2017), and due to deposition of atmospheric
60 N, coming mostly from fossil fuel combustion (Holland et al., 1999). These large N in-
61 puts to soils have not been balanced by N removal from soils through incorporation into
62 plant biomass and crop harvest, resulting in large soil N surpluses in many places across
63 the world, e.g. in the US (Byrnes et al., 2020), in Europe (Erisman et al., 2011) and in
64 China (X. Wang et al., 2014). Furthermore, wastewater can be released to the environ-
65 ment with or without treatment, which constitutes a point source of N (United Nations,
66 2017). In Europe, the efficiency of wastewater treatment plants has largely improved since
67 1990 (European Commission, 2020). Nevertheless water bodies still receive large point N
68 loads, and for many countries, further enhancement of treatment facilities are prescribed
69 (European Commission, 2020; Svirejeva-Hopkins et al., 2011).

70 This excess of N in the environment has substantial consequences for both the hydro-
71 sphere and the atmosphere (Robertson & Groffman, 2015). In fact, soluble N compounds,
72 and more specifically nitrate, are polluting drinking water, which threatens human health
73 (WHO, 2016). They are also causing eutrophication of receiving water bodies, such as Euro-
74 pean seas (EEA, 2019b) and coastal areas in the US (Scavia & Bricker, 2006). In addition,
75 denitrification in the terrestrial system, which microbially reduces nitrate, can release large
76 amount of nitrous oxide (N_2O) (Tian et al., 2018). The latter is an important greenhouse
77 gas almost 300 times as potent as CO_2 (Myhre et al., 2013), and contributes to the depletion
78 of stratospheric ozone (Portmann et al., 2012). Therefore, reducing nitrate levels through
79 improved land management strategies is a pressing issue, in particular in Europe where
80 countries such as France, Germany and Greece have been recently fined by the European
81 Court of Justice for exceeding the regulatory limits for nitrate in receiving water bodies
82 (Damania et al., 2019).

83 Sporadic evidence shows that N inputs to the soil can not only reach surface water
84 bodies or be lost to the atmosphere via denitrification, but they can also accumulate in the
85 landscape as legacy N (Chen et al., 2018; Van Meter & Basu, 2015). A few studies including
86 long-term measurements of soil N content in the Mississippi River Basin (Van Meter et al.,
87 2016), fertilization experiments in the UK and in France (Jenkinson, 1991; Sebilo et al.,
88 2013) and mass balance assessments (Smil, 1999; Worrall et al., 2015) suggest that part
89 of the N surpluses can build up in the root zone of agricultural soils in organic forms
90 (biogeochemical legacy). Furthermore, increasing nitrate concentration trends are detected
91 in groundwater in some locations in the US and the UK (Puckett et al., 2011; Stuart et
92 al., 2007). The pervasive issue of nitrate pollution in groundwater, in particular in Europe
93 (Sundermann et al., 2020; EEA, 2018), and the results of modelling studies focusing on
94 N accumulation in the vadose zone (Ascott et al., 2017; L. Wang et al., 2012) points to a
95 widespread buildup of N in dissolved inorganic forms (hydrologic legacy). Biogeochemical
96 and hydrologic legacies can impact the future water quality status of water bodies. They
97 can induce a delay or “time lag” between changes in land management practices and the
98 water quality response (Grimvall et al., 2000; Vero et al., 2018). The implications of the
99 two legacy forms for future water quality could be very different because hydrologic legacy
100 corresponds to the accumulation of reactive and mobile N, and biogeochemical legacy to the
101 accumulation of much more stable (organic) N compounds. Therefore, a characterization of
102 both types of N legacies at catchment scale is crucial to inform the design of effective water
103 quality measures.

104 However, our understanding of the magnitude of these legacies and their associated
105 timescale remains limited because of a lack of observational data and the uncertainties
106 associated with N legacy modelling. Direct observational data of N content in soil and
107 groundwater are often sparse in time and space. This makes it difficult to capture the
108 temporal changes and spatial variability in N content and to determine the integrated legacy
109 behaviour at catchment scale. In particular, large-scale datasets of soil N content are often
110 available for one year (e.g. Ballabio et al., 2019). Regarding groundwater N concentration
111 measurements, in Europe, low-frequency (typically annual) measurements and the fact that
112 they are mostly available for the recent years impedes the analysis of the long-term dynamics.
113 Additionally, assessing the spatial distribution of groundwater concentration from point
114 measurements involves large uncertainties (see e.g. Figure 6 in Knoll et al., 2020). Therefore,
115 mechanistic models should be used to quantify N legacies, to complement the information

116 provided by currently available observation data of N content in soil and groundwater that
117 are insufficient.

118 In this respect, some past modelling studies investigate the time lag between the tra-
119 jectory of N inputs to the terrestrial system and the in-stream N levels using empirical
120 approaches, e.g. the studies of Chen et al. (2014), Dupas et al. (2020), Ehrhardt et al.
121 (2021) and Van Meter and Basu (2017) (further details are reported in the review of Chen
122 et al., 2018). Yet, such modelling approaches are typically based on lumped transfer func-
123 tions that relate the N inputs to the N stream export at catchment scale and they do not
124 explicitly disentangle the role of biogeochemical and hydrologic legacies. Only few stud-
125 ies, all of them focusing on North America, explicitly consider and examine both types of
126 N legacies at catchment scale using mechanistic models, namely a modified version of the
127 Soil Water Assessment Tool model (SWAT-LAG, Ilampooranan et al., 2019), the NOAA’s
128 Geophysical Fluid Dynamics Laboratory Land Model (LM3-TAN, Lee et al., 2016), and
129 the more parsimonious Exploration of Long-tErM Nutrient Trajectories model (ELEMNT,
130 Chang et al., 2021; J. Liu et al., 2021; Van Meter et al., 2017, 2018).

131 Importantly, the investigation of N legacies through modelling approaches is fraught
132 with large uncertainties. First, the N input data have large uncertainties because their
133 construction involves numerous uncertain factors, as reported in Byrnes et al. (2020),
134 Häußermann et al. (2020), Hong et al. (2012), Poisvert et al. (2017), and Häußermann
135 et al. (2020) for diffuse N sources and in Grizzetti et al. (2008), Morée et al. (2013), and
136 Van Meter et al. (2017) for point sources (wastewater). Notably, although the application
137 of mineral fertilizer is a key N input to agricultural soils, data may only be available at the
138 national level for some countries such as Germany, and spatial disaggregation strategies have
139 to be developed to estimate fertilizer application at finer spatial resolutions (Häußermann et
140 al., 2020). Second, the modelling of N legacies suffers from a lack of process understanding,
141 e.g. regarding the immobilization and accumulation of N into organic matter in soils (see
142 e.g. Bingham & Cotrufo, 2016; Yansheng et al., 2020). Third, the parameters of mechanis-
143 tic N models are generally estimated through calibration (Moriassi, Zeckoski, et al., 2015),
144 because they are often conceptual parameters that cannot be directly related to measurable
145 quantities. Parameter values are typically constrained using in-stream measurements only
146 (Moriassi, Zeckoski, et al., 2015), since observational data of internal model variables, such
147 as N content in soil and groundwater, are generally lacking. It is well known that different
148 parameter sets can fit the in-stream data equally well, as discussed in previous water quality

149 studies, e.g. Ford et al. (2017), Husic et al. (2019), Rankinen et al. (2006), and Wade et al.
150 (2008). Because of this issue of equifinality (Beven, 2006), it may be possible to identify a
151 range of plausible values for the model internal fluxes and states corresponding to the differ-
152 ent plausible parameter sets. Hence, simulated N legacies (internal model states) might be
153 poorly characterized if in-stream information only is used to constrain model parameteriza-
154 tions. All of the discussed uncertainties in N legacy modelling are exacerbated by the fact
155 that the N accumulation in the landscape needs to be modelled over long timescales (decades
156 to centuries) to understand the contemporary and future water quality status. In fact, long
157 time series of input data are fraught with uncertainties and long records of observations of
158 model outputs, such as in-stream N concentrations, are rarely available.

159 Our review of the literature suggests that 1) we lack understanding of the magnitude
160 and timescale of N legacies at catchment scale in light of the associated uncertainties and 2)
161 it remains unclear whether and to what extent the in-stream information only, as typically
162 used to calibrate catchment-scale N water quality models, is able to constrain the simulated
163 N legacies and which additional information would mostly help to reduce uncertainty. In
164 this study, we address these gaps by investigating the long-term fate of the N inputs to the
165 landscape and its uncertainties. In particular, we analyze the uncertainties in simulated N
166 biogeochemical and hydrologic legacies due to the uncertainties in the model parameters
167 and the input data, and we determine the value of different types of (observational) data to
168 constrain the modelling results.

169 To this end, first, we introduce a multicriteria approach based on soft rules to constrain
170 the model parameters, which allows assessment of parameter uncertainty and of the value
171 of the different observational data available (in-stream N loading and concentration data,
172 and soil N data). Secondly, we perform a sensitivity analysis to determine the factors
173 responsible for the (residual) uncertainty in the simulated N legacies to prioritize future
174 efforts for uncertainty reduction and model improvement. We apply the ELEMENNT model,
175 which is a parsimonious N model that explicitly accounts for both biogeochemical and
176 hydrologic legacies (Van Meter et al., 2017). While past modelling studies focus on North
177 America (Chang et al., 2021; Ilampooranan et al., 2019; Lee et al., 2016; J. Liu et al., 2021;
178 Van Meter et al., 2017, 2018), here we extend the analyses of N legacies to the European
179 context. We examine the N legacy behaviour over the last six (1960–2015) decades in
180 the Weser river basin (WRB), which is Germany’s largest national river basin. Through
181 the application of the soft rules and the sensitivity analysis, we infer the dominant factors

182 affecting the uncertainty in simulated N legacies and discuss the implications for future
183 modelling studies, data monitoring, and water and land management strategies.

184 **2 Model description**

185 The ELEMeNT model (Van Meter et al., 2017) simulates the fate of the diffuse N
186 sources (soil N surplus) and point sources at annual timescale and it computes the an-
187 nual in-stream nitrate-N loading and concentration at the catchment outlet. The model
188 assumes that dissolved N is present in the form of nitrate (NO_3). ELEMeNT conceptualizes
189 the N processes in two terrestrial compartments, a shallower compartment referred to as
190 “source zone”, which represents the soil root zone (assumed to have a depth of 1 m), and a
191 deeper compartment referred to as “subsurface zone”, which includes both the unsaturated
192 zone below the source zone and the groundwater. The land use categories considered are
193 cropland, agricultural permanent grassland, and non-agricultural land (see Section 3.2.1).
194 ELEMeNT requires as input the annual time series of the different land use fractions, the N
195 surplus for each land use category, the stream discharge at the catchment outlet, and the N
196 point sources. We revise the formulation of the subsurface submodel and add an in-stream
197 submodel as detailed in Sections 2.2 and 2.3. The model version used in this study counts
198 nine calibration parameters (Table 1).

Table 1. Description of the ELEMNT Model Parameters, Ranges Used in this Study, and References for the Determination of the Ranges

Parameter	Description	Unit	Lower value	Upper value	References for the values
$M_{s_{org}}^{prist}$	Source zone organic N stock under pristine conditions	($kg\ ha^{-1}$)	10^4	3.5×10^4	The range includes the estimates of soil N content in 2009 from LUCAS dataset (Ballabio et al., 2016, 2019)
h_c	N protection coefficient for cultivated land	(-)	0.1	0.5	Van Meter et al. (2017, Table S2.1); Chang et al. (2021, Table S3)
h_{nc}	N protection coefficient for non-cultivated land	(-)	0.25	0.75	Van Meter et al. (2017, Table S2.1); Chang et al. (2021, Table S3)
k_a	Mineralization rate constant for organic active N store	(yr^{-1})	0.05	0.75	The range includes the values in Van Meter et al. (2017, Table S2.1)
V_s^a	Mean annual water content in the source zone	(mm)	100	500	Van Meter et al. (2017, Table S2.1)
λ_s	Denitrification rate constant in the source zone	(yr^{-1})	0.1	1	Van Meter et al. (2017, Table S2.1)
λ_{sub}	Denitrification rate constant in the subsurface zone	(yr^{-1})	0.01	0.3	Van Meter et al. (2017, Table S2.1); Puckett et al. (2011); Heidecke et al. (2015, Sect. 3.2.3.2)
μ_{sub}	Mean travel time in the subsurface	(yr)	2	50	Van Meter et al. (2017, Table S2.1); Koeniger et al. (2008, Table 2)
R^b	Fraction of in-stream N removal	(-)	0.01	0.3	Howarth et al. (1996, Table 9); Mulholland et al. (2008, Figure 4.c); X. Yang et al. (2018); Grizzetti et al. (2008, Table 6)

^a V_s integrates the parameters for the porosity, saturation and depth of the source zone reported in Van Meter et al. (2017).

^b R is a new parameter for in-stream processes, introduced in this study.

2.1 Source Zone Submodel

Following Van Meter et al. (2017), the model assesses the dynamics of the organic N pool, accounting for the biogeochemical legacy, and of the inorganic N pool. The organic N pool is divided into two different stores: (1) a protected N store with a slow turnover, that accounts for the physical stabilization of N, and (2) an active organic N store, that consists of organic N which is more labile and prone to mineralization. The organic N stores receive the total N surplus. Therefore mineralization in the model (the simulated N mass flux from the organic to the inorganic pool) represents the effective N mass flux to the inorganic N pool. This flux results from the combined effect of the transformation of organic N into mineral forms and the immobilization of mineral N inputs into the organic matter. Immobilization is understood to be an important process in both agricultural soils (Blankenau et al., 2001; Haag & Kaupenjohann, 2001; X. Liu et al., 2016; Macdonald et al., 1989; Sebilo et al., 2013; Yansheng et al., 2020) and forested soils (Castellano et al., 2012; Lewis & Kaye, 2012; Morier et al., 2008; Spoelstra et al., 2001). However, these process interactions are yet not well understood (Bingham & Cotrufo, 2016; Yansheng et al., 2020) and therefore difficult to represent explicitly in a mechanistic model. Since mineralization is parameterized as a first order process, part of the N surplus is quickly transferred to the inorganic N store and can therefore be readily available for leaching. A protection coefficient determines the fraction of the N surplus that is added to the protected store. Transfer of N mass from the protected to the active N stores occurs in case of land use conversion from uncultivated land to cropland. After mineralization occurs, the inorganic N in the source zone can either denitrify or leach to the subsurface.

2.2 Subsurface Submodel

In the subsurface, the transport of dissolved inorganic N is represented using a travel time distribution to account for hydrologic legacy, while N can denitrify following a first order process (Van Meter et al., 2017). In this study, we revise the formulation for the subsurface compartment. Compared to the previous model formulation (Van Meter et al., 2017), the travel time distribution function is an explicit function of time t (Benettin et al., 2015; Botter et al., 2010; Quéloz et al., 2015). The N-NO₃ export from the subsurface to the stream $J_{stream_{sub}}(t)$ ($kg\ ha^{-1}\ yr^{-1}$) at time t is therefore written as:

$$J_{stream_{sub}}(t) = \int_0^{+\infty} J_{sub_s}(t-T)p(T, t-T)e^{-\lambda_{sub}T}dT \quad (1)$$

230 where T (yr) is the travel time, J_{sub_s} ($kg\ ha^{-1}\ yr^{-1}$) is the N-NO₃ mass leaching from
 231 the source zone to the subsurface, $p(T, t)$ (-) is the travel time distribution function and
 232 λ_{sub} (yr^{-1}) is the rate constant of denitrification in the subsurface. As in Van Meter et al.
 233 (2017), we assume complete mixing (or random sampling) in the subsurface compartment
 234 and we adopt an exponential distribution for the travel time (Equation 41 in Botter et al.,
 235 2010). The mean value of the distribution $\mu'(t)$ (yr) is given as:

$$236 \quad p(T, t - T) = \frac{1}{\mu'(t)} e^{-\int_{t-T}^t \frac{1}{\mu'(x)} dx} \quad (2)$$

237 with

$$238 \quad \mu'(t) = \frac{\overline{Q_{out}\mu_{sub}}}{Q_{out}(t)} \quad (3)$$

239 where $Q_{out}(t)$ ($mm\ yr^{-1}$) is the discharge at the catchment outlet, $\overline{Q_{out}}$ ($mm\ yr^{-1}$) is
 240 the arithmetic mean of the discharge, and μ_{sub} (yr) is the harmonic mean of $\mu'(t)$. To account
 241 for the fact that the mean discharge may not be stationary, we compute $\overline{Q_{out}}$ at each time
 242 step as the 30-year backward moving average of the discharge. We refer to supplementary
 243 Sections S1-S3 for further details on the mathematical derivation and numerical integration
 244 of the new equations introduced in this study.

245 **2.3 In-stream Submodel**

246 In-stream N removal, which comprises the processes of denitrification and biotic as-
 247 similation described e.g. in Basu et al. (2011) and Dehaspe et al. (2021), was implicitly
 248 accounted for in Van Meter et al. (2017). The removal of N from point sources was lumped
 249 with the removal due to wastewater treatment, and the removal of N from diffuse sources
 250 was lumped with the denitrification in the terrestrial compartments. In this study, we need
 251 to represent in-stream removal explicitly, since our point N sources input, described in Sec-
 252 tion 3.2.4, already includes the N removal through wastewater treatment. The in-stream
 253 NO₃-N load $J_{out}(t)$ ($kg\ ha^{-1}\ yr^{-1}$) is computed as:

$$254 \quad J_{out}(t) = (J_{stream_{sub}}(t) + J_{ps}(t))R \quad (4)$$

255 where R (-) is the annual fraction of in-stream N removal and $J_{ps}(t)$ ($kg\ ha^{-1}\ yr^{-1}$)
 256 is the N loading from point sources. For our application at catchment scale and annual
 257 timescale, we thereby assume that in-stream N removal can be represented by a first order
 258 process, as documented e.g. in Basu et al. (2011).

3 Study Catchments and Data

3.1 Description of the Study Catchments

We apply the ELEMeNT model to the Weser river basin (WRB) in Germany, focusing on the region located upstream of the Hemelingen station (see Figure 1a, b). This covers an area of around 38,450 km^2 , which corresponds to almost 11% of the total area of Germany. The Weser river largely contributes to the total N load discharging into the North Sea, where eutrophication is a major issue (Arle et al., 2017). In the WRB, a priority goal set by the WRB Commission (FGG Weser, 2020) is to reduce N inputs to the landscape to achieve in-stream N concentrations below the regulatory threshold of 2.8 $mg L^{-1}$ (OGewV, 2016). For our analyses, we selected eight stations, including Hemelingen, that have a long record (between 26 and 37 years) of 14-days average in-stream nitrate measurements, that were constructed by mixing daily samples. These stations are situated on the Weser, Werra, Fulda and Aller rivers and their location is reported in Figure 1b.

The WRB is characterized by a humid temperate climate with an annual mean precipitation around 780 $mm yr^{-1}$ (spatial range: 600–1100 $mm yr^{-1}$) and a mean aridity index (ratio of potential evapotranspiration to precipitation) around 0.9 (S. Yang et al., 2019; Zink et al., 2017). The average annual discharge at Hemelingen over the period 1950–2015 amounts to 268 $mm yr^{-1}$. Agriculture is the dominant land use type and constitutes 45% of the catchment area in 2015 (35% cropland and 10% agricultural permanent grassland). Other important land uses are forested land and other vegetated land (including natural grassland and urban green areas), which cover 34% and 19% of the catchment area in 2015, respectively. Spatially and temporally averaged annual N surplus is estimated to be equal to 48.6 $kg ha^{-1} yr^{-1}$ over the period 2011–2015, and N surplus takes a higher value over agricultural areas (70.9 $kg ha^{-1} yr^{-1}$) compared to non-agricultural areas (30.3 $kg ha^{-1} yr^{-1}$). On average in-stream N- NO_3 concentration (C_{out}) value at the catchment outlet is equal to 3.7 $mg L^{-1}$ over the period 2011–2015, which is above the target value of 2.8 $mg L^{-1}$ (OGewV, 2016).

The eight nested subcatchments analyzed in this study, present some moderate differences in their characteristics, as indicated in Figure 1c-j. In particular, the percentage of agricultural areas ranges from 38% to 48%, with lower values in the southern (upstream) part, which is situated in a mountainous area, compared to the northern (downstream) part, which lies in the German Northern Plain. We notice a sharp decrease in N surplus in 1990

291 for the Letzter Heller subcatchment (Figure 1j). This can be explained by the fact that a
292 large area of the subcatchment is situated within the state of Thuringia, which was part of
293 the former German Democratic Republic, and where agricultural activities were profoundly
294 disrupted following the German reunification in 1990. The in-stream concentration C_{out}
295 ranges from 3.0 mg L^{-1} at the Wahnhausen station (Figure 1i), which is located in the up-
296 stream part, to 4.1 mg L^{-1} at the downstream Drakenburg and Porta stations (Figure 1d,
297 f).

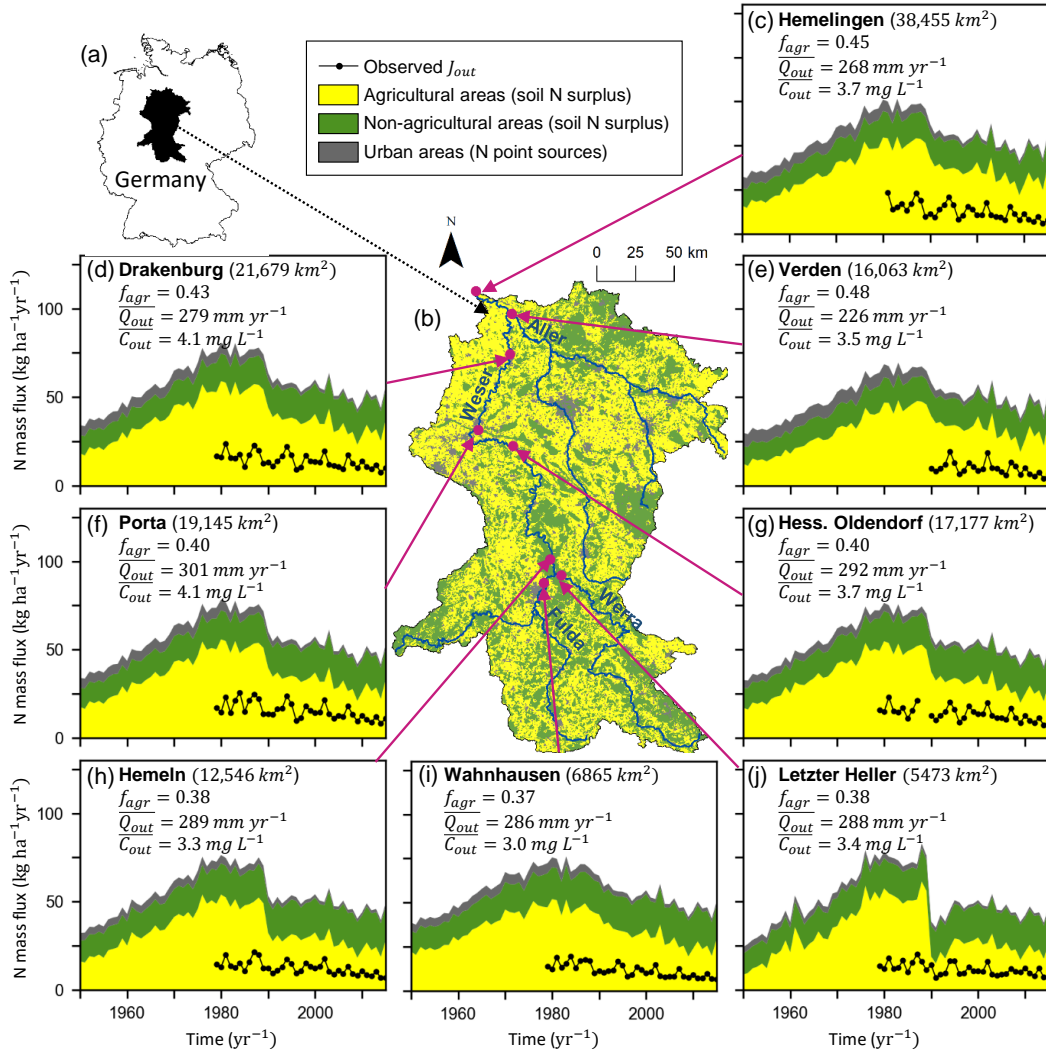


Figure 1. The eight subcatchments of the WRB selected for the analyses: (a) location of the WRB in Germany, (b) land use of the WRB and outlet of the subcatchments analyzed, and (c-j) N input (N surplus and N point sources), in-stream observations (N-NO₃ loading, J_{out}) time series for the period 1950–2015, and catchment properties namely catchment area, fraction of agricultural area in 2015 (f_{agr}), average annual stream discharge over the period 1950–2015 ($\overline{Q_{out}}$), and average observed in-stream N-NO₃ concentration over the period 2011–2015 ($\overline{C_{out}}$). Source of the land use data in panel (b): Corine Land Cover data for year 2012 (EEA, 2019a). Other datasets used are described in Section 3.2.

3.2 Data Description and Processing

In this section, we present the datasets adopted to run ELEMeNT and the datasets of N content observations used to assess the performance of the model and estimate its parameters (as explained in Section 4).

3.2.1 Land Use Data

We construct the 1800–2015 trajectories of the catchment-scale fractions of the three land use categories required by ELEMeNT, namely cropland, agricultural permanent grassland and non-agricultural land. The latter land cover includes forest, other vegetated land (such as natural grassland, green urban areas), built-up areas and non-vegetated land. We combine data from the gridded Corine Land Cover dataset (CLC; EEA, 2019a), the gridded History Database of the Global Environment dataset (HYDE; Klein Goldewijk et al., 2011, 2017) and census data on agricultural areas available from the Federal Statistical Office (Statistisches Bundesamt, 2021) and from the yearly statistical books for Germany (Digizeitschriften, 2021). Supplementary Section S4 provides details on the methodology used to construct the land use data. The trajectories of the land use fractions for the different subcatchments are presented in supplementary Figure S1.

3.2.2 N Surplus for Agricultural Areas

We adopt the N surplus dataset for agricultural areas of Häußermann et al. (2020), which is available for the period 1995–2015 at the county level, and the dataset of Behrendt et al. (2003), which is available for the period 1950–1998 at the state level, and which builds on the studies of Bach and Frede (1998) and Behrendt et al. (2000). The components included in the two datasets are the N content in the input of mineral fertilizer, manure, other organic fertilizer such as sewage sludge, seeds and planting material (for the county level dataset only), atmospheric deposition, biological fixation by legumes, as well as the N content in harvested crops. We refer to Häußermann et al. (2020) and Behrendt et al. (2003) for further methodological details. We harmonize the two N surplus datasets similar to Ehrhardt et al. (2021), to construct the N surplus trajectories at county level for the period 1950–2015 (see Supplementary Section S5 for further details). The resulting trajectories of the N surplus for agricultural areas are shown in supplementary Figure S2.

3.2.3 *N Surplus for Non-agricultural Areas*

Following Van Meter et al. (2017), for non-agricultural areas, we consider two components for the N surplus, namely atmospheric N deposition and biological N fixation, and we neglect any net accumulation of N in the vegetation. We quantify atmospheric N deposition using the dataset produced from Community Atmosphere Model with Chemistry (CAM-chem, Lamarque et al., 2012) simulations, as part of the National Center for Atmospheric Research (NCAR) Chemistry-Climate Model Initiative (CCMI, Tilmes et al., 2016) N deposition dataset. This product is part of the input datasets for the Model Intercomparison Projects (input4MIPS) and it is a forcing dataset for the Coupled Model Intercomparison Project phase 6 (CMIP6, Eyring et al., 2016). The data are provided over a $1.9^\circ \times 2.5^\circ$ grid for the period 1850–2014. We estimate biological N fixation using the mean annual rate reported by Cleveland et al. (1999) for natural temperate forest ($16 \text{ kg ha}^{-1} \text{ yr}^{-1}$) and for natural grassland ($2.7 \text{ kg ha}^{-1} \text{ yr}^{-1}$). We use the latter for our land use category “other vegetated land” defined in Section 3.2.1. The trajectories of atmospheric N deposition and biological N fixation are shown in supplementary Figure S3.

3.2.4 *N Point Sources*

For N point sources, we use observations of N loading, available for 802 wastewater treatment plants (WWTPs) and one year in the period 2012–2016 depending on the plants (S. Yang et al., 2019; Büttner, 2020). Data for the larger WWTPs (with population equivalent over 2,000) come from the Environmental Agency database (EEA, 2015) and correspond to the year 2012, while data for the smaller WWTPs (with population equivalent under 2,000) come from the authorities of the federal German states and correspond to the year 2015 or 2016. For the past years, we estimate N point sources from wastewater from the methodology proposed by Morée et al. (2013). We utilize data on population count (HYDE dataset), protein supply (FAO, 1951, 2021a, 2021b), and population connection to sewer and WWTPs (Seeger, 1999; Eurostat, 2016, 2021). We combine these data and create an ensemble of historical N loading from WWTPs over the period 1950–2015. The ensemble reflect the uncertainty in the characteristics of different parameters, such as the fraction of protein supply lost in the food supply chain, the ratio of industrial to domestic N emissions or the efficiency of wastewater treatment. Supplementary Section S6 (as well as Figure S4 and Tables S1-S2) details the underlying procedure for the N point sources construction. A visual depiction of the N point sources with uncertainty is provided in Figure S5.

3.2.5 Stream Discharge

To run the ELEM_ENT model, we require annual discharge at the outlet of the sub-catchments for the period 1800–2015 and, in addition, we need daily discharge for the recent period to process the measurements of in-stream N-NO₃ concentration, as described in Section 3.2.6. Discharge data is constructed by combining (1) daily discharge measurements (at the catchment outlet or at a nearby measuring station) obtained from the GRDC (Global Runoff Data Centre, 2021) or the WRB Commission (FGG Weser, 2021) databases (see supplementary Table S3), and (2) bias-corrected simulations from the mesoscale Hydrologic Model (mHM, Kumar et al., 2013; Samaniego et al., 2010), to fill the missing values in the observation dataset. Two sets of mHM simulations are used, medium-term daily simulations for the period 1950–2015 (Zink et al., 2017), and long-term annual simulated values for the period 1800–1949 (Hanel et al., 2018). The mHM simulations capture the variability of observed discharge reasonably well, with values of the Nash–Sutcliffe efficiency always higher than 0.64 and values of the coefficient of determination always higher than 0.66 (see supplementary Table S4). Figures S6–S13 represent the annual time series of the discharge measurements and the simulations before and after we apply the bias-correction. We refer to Zink et al. (2017) and Hanel et al. (2018) for details on the mHM setups.

3.2.6 Observations of N Content

N content in the Source Zone

We derive N content in the topsoil (0–20 cm) from the Land Use and Cover Area frame statistical Survey (LUCAS; Ballabio et al., 2016, 2019). The LUCAS dataset was created from the spatial interpolation of approximately 22,000 surveyed points across Europe. For most countries, including Germany, soil samples were collected in 2009. To estimate the catchment-scale soil N content (0–100 cm, source zone of ELEM_ENT), we combine the N content and bulk density of the topsoil from the LUCAS dataset. We also use the ratio of total soil N content (0–100 cm) to topsoil N content (0–20 cm), which we estimate to be between 2.5 and 4 from Batjes (1996), thus obtaining a plausible range for the total soil N content (0–100 cm). Our estimated ranges of the soil N content and further details are reported in supplementary Table S5.

In-stream N Concentration

389 In-stream nitrate concentration is obtained from the WRB Commission (FGG Weser,
 390 2021). For the Letzter Heller catchment, we combine the concentration measurements at
 391 the Letzter Heller station available for the period 1979–2002 and at the Witzenhausen
 392 station, which is located 8 km upstream, for the period 2003–2015. The data consists of
 393 14-day average N- NO_3 concentration measurements, that were constructed by mixing daily
 394 samples, and that start for most stations in the early 1980s and end around 2015. We only fill
 395 the gaps that have a length of maximum 42 days, and therefore concentration data for years
 396 containing longer gaps are discarded. Annual total in-stream loading is calculated as the
 397 sum of the 14-day average loading values, while annual average concentration is estimated
 398 as the discharge weighted average of the 14-day average concentration values. The in-stream
 399 N- NO_3 concentration and loading data are reported in supplementary Figures S14–S15. We
 400 also examine the uncertainty in the observations and check for outlier values. We find that
 401 the concentration value at the Letzter Heller station in 1990, which is equal to 6.3 mg L^{-1} ,
 402 is abnormally high. The difference to the average value (4.5 mg L^{-1}) amounts to 2.8 times
 403 the standard deviation over the period 1985–1995 (see supplementary Figure S14). This
 404 anomalous concentration value could be explained in the context of the German reunification
 405 in 1990, where unusual and undocumented N amounts could have been discharged into the
 406 stream. This is not reflected in our N input datasets. Tracking the cause of this anomaly is
 407 beyond the scope of this study, and therefore, we discard this value for our analyses.

408 **4 Methods for Parameter Estimation and Sensitivity Analysis**

409 **4.1 Multicriteria Parameter Estimation Strategy**

410 Our parameter estimation strategy considers the performance of the ELEM_eNT model
 411 in simulating three different variables, namely the total source zone N content (M_s , which
 412 includes the organic protected, organic active, and inorganic N stores), and the in-stream
 413 N- NO_3 loading (J_{out}) and concentration (C_{out}) at the catchment outlet. Regarding M_s ,
 414 the simulated values are constrained within the range derived from the observations, since
 415 the source zone N content is only provided for the year 2009. For J_{out} and C_{out} , we use
 416 three performance metrics that are the Pearson correlation coefficient denoted as ρ (-), the
 417 relative bias denoted as $RBIAS$ (-) and the variability error denoted as STD_{err} (-). $RBIAS$
 418 and STD_{err} are defined as follows:

$$419 \quad RBIAS = \frac{\mu_{sim} - \mu_{obs}}{\mu_{sim}} \quad (5)$$

420
421

$$STD_{err} = \frac{\sigma_{sim} - \sigma_{obs}}{\sigma_{sim}} \quad (6)$$

422
423
424
425
426
427
428

where μ_{obs} and μ_{sim} are the average of the observations and simulations, respectively, and σ_{sim} and σ_{obs} are the standard deviation of the simulations and observations, respectively. These averages and standard deviations are calculated for each subcatchment over the years where observations are available. The three metrics ρ , $RBIAS$ and STD_{err} measure how well the dynamics (temporal pattern and timing), the mean and the variability of the observations respectively are captured by the simulations. They constitute the three components of the Kling-Gupta efficiency (KGE ; Gupta et al., 2009) defined as:

429

$$KGE = 1 - \sqrt{(1 - \rho)^2 + RBIAS^2 + STD_{err}^2} \quad (7)$$

430
431
432

We consider these three metrics separately instead of the aggregated KGE measure to ensure a sufficient performance with regards to all important aspects that we aim to simulate, as discussed in Martinez and Gupta (2010).

433
434
435
436

Similar to e.g., Choi and Beven (2007), Hartmann et al. (2017), (Husic et al., 2019), and Sarrazin et al. (2018), we use “soft rules” to identify the set of well-performing (“behavioural”) simulations. We define seven soft rules, all of which have to be satisfied in the behavioural simulation ensemble:

437
438
439
440
441
442
443

1. for J_{out} : $|RBIAS| \leq 0.2$;
2. for J_{out} : $|STD_{err}| \leq 0.25$;
3. for J_{out} : $\rho \geq 0.8$;
4. for C_{out} : $|RBIAS| \leq 0.2$;
5. for C_{out} : $|STD_{err}| \leq 0.25$;
6. for C_{out} : $\rho \geq 0.6$;
7. the simulated M_s is within the range derived from the observations.

444
445
446
447
448
449
450

The order of the rules allows us to assess to what extent the use of in-stream N concentration and source zone N content data can help to reduce the simulation uncertainties, beyond the use of in-stream N loading data. Some studies only examine the in-stream N loading (e.g. Chang et al., 2021; J. Liu et al., 2021; Van Meter et al., 2017, 2018) and not the in-stream N concentration that tends to be more difficult to simulate than the in-stream N loading (Husic et al., 2019). In addition, as discussed in Section 1, previous studies generally considered in-stream variables only for calibration. The threshold values

451 for *RBIAS* and ρ introduced in rules 1, 3, 4 and 6 correspond to “satisfactory” or “good”
452 model performance in reproducing nutrient dynamics according to Moriasi, Gitau, et al.
453 (2015). We however note that Moriasi, Gitau, et al. (2015) examine values of ρ at monthly
454 and not annual timescale, due to a lack of studies analysing the model goodness-of-fit for
455 annual simulations of nutrients. Here, we set a stricter threshold value on ρ for J_{out} (rule
456 3) compared to C_{out} (rule 6), since the dynamics of J_{out} are driven by the stream discharge
457 and are therefore easier to reproduce than the dynamics of C_{out} , as further discussed in
458 Sections 5.1.1-5.1.2. Due to a lack of analysis of STD_{err} in previous studies, we consider
459 that a threshold value equal to ± 0.25 is reasonable (rules 2 and 5).

460 To estimate the nine model parameters, we generate a parameter sample of size 100,000
461 from the ranges reported in Table 1 utilizing latin hypercube sampling and uniform distri-
462 butions. We discard the parameter sets that do not meet the condition $h_c < h_{nc}$ (where
463 h_c and h_{nc} are the protection coefficients for cultivated and non-cultivated land, respec-
464 tively). We assume that the protection of organic matter is reduced by tillage practices. We
465 perform Monte-Carlo simulations for each of the eight subcatchments and we sequentially
466 apply the seven soft rules, thus progressively reducing the number of behavioural parameter
467 sets. Following previous studies (Dupas et al., 2020; Ehrhardt et al., 2021; Van Meter et
468 al., 2017), we use the entire time series of in-stream N observations to identify behavioural
469 simulations. We note that the goal of our analysis here is not to predict future catchment N
470 export but to analyze the uncertainty in the simulations and the value of different types of
471 data to constrain the simulations. In addition, the amount of in-stream observational data
472 available (between 26 and 37 years depending on the subcatchments) is rather limited to be
473 divided between a calibration set and an independent verification set.

474 We simulate the ELEMENNT model from year 1800 (pre-industrial conditions) to year
475 2015, including a long warm-up period i.e., we only analyze the simulations for the period
476 1960–2015 and we discard the results for period 1800–1959. This is because the legacy stores
477 can have a slow turnover and can build up over long timescales (Van Meter et al., 2017).
478 The setup of the initial states is described in detail in supplementary Section S7. Regarding
479 the N point sources, we select the realization in our ensemble that shows the best match
480 with the observations available for the period 2012–2016 (further information on the point
481 sources are in Section 3.2.4). For the atmospheric N deposition, we use the value in 1850
482 for the period 1800–1849. Regarding the N surplus in agricultural areas, since no data are
483 available before 1950, we assume that the value (at county level) of the N surplus in 1850

484 is half the value in 1950. We then use linear interpolation for the period 1850–1950 and
 485 we consider that the value is constant for the period 1800–1850. We also assume that the
 486 N surplus takes the same value over cropland and agricultural permanent grassland. In
 487 Section 4.2, we explain how we assess the impact of the uncertainty in the N point sources
 488 and N surplus.

489 4.2 Sensitivity Analysis of the Simulated N Legacies

490 We perform a sensitivity analysis to investigate the factors that are responsible for the
 491 residual uncertainty in the simulated N legacy stores, i.e., the uncertainty that remains after
 492 constraining the model simulations using the soft rules described in Section 4.1. This analysis
 493 allows us to set priorities for future efforts for uncertainty reduction and model improvement.
 494 We examine the sensitivity of four model outputs related to the legacy stores (namely the
 495 average source zone and subsurface storage and their cumulative change, assessed over the
 496 period 1960–2015) to the nine parameters of ELEMeNT, the N point sources input and the
 497 N surplus input. We select ten realizations of the N point sources across the ensemble of
 498 realizations to cover the uncertainty range (see Figure S5). Regarding the N surplus, we
 499 introduce two additional parameters to generate alternative realizations for the agricultural
 500 N surplus for the period (1800–1949) and for the disaggregation between cropland and
 501 agricultural permanent grassland. First, we define parameter r_{warm} (-), which represents
 502 the ratio of the value in 1850 to the value in 1950 of the agricultural N surplus $Surplus_{agr}(t)$
 503 ($kg\ ha^{-1}\ yr^{-1}$):

$$504 \quad r_{warm} = \frac{Surplus_{agr}(1850)}{Surplus_{agr}(1950)} \quad (8)$$

505 The agricultural N surplus for the period 1800–1949 is derived from r_{warm} , through
 506 linear interpolation over the period 1850–1950 and by setting a constant value over the
 507 period 1800–1850. Second, we define parameter $r_{mgra-crop}$ (-), which is the ratio of the
 508 N surplus for permanent agricultural grassland $Surplus_{mgra}(t)$ ($kg\ ha^{-1}\ yr^{-1}$) to the N
 509 surplus for cropland $Surplus_{crop}(t)$ ($kg\ ha^{-1}\ yr^{-1}$), assumed to be constant in time:

$$510 \quad r_{mgra-crop} = \frac{Surplus_{mgra}(t)}{Surplus_{crop}(t)} \quad (9)$$

511 In addition, we define a time-invariant multiplier denoted as $f_{surplus}$ (-), which is used to
 512 multiply the time series 1800–2015 of the N surplus for both agricultural and non-agricultural
 513 areas. This multiplier accounts for the uncertainty in the value of the total N surplus.

514 We select three values for $f_{surplus}$ (0.8, 1 and 1.2), r_{warm} (0.25, 0.5 and 0.75) and
 515 $r_{mgra-crop}$ (0.5, 1 and 1.5), which results in 27 N surplus realizations. Since no informa-
 516 tion is available to further constrain the uncertainty, we argue that these 27 realizations
 517 cover a large plausible range of N-surplus estimates. The case $f_{surplus} = 1$, $r_{warm} = 0.5$
 518 and $r_{mgra-crop} = 1$ corresponds to our “baseline scenario” i.e., the one used for analyses
 519 presented in Section 4.1. Supplementary Section S8 details the derivation of the N surplus
 520 for cropland and permanent agricultural grassland from the parameter $r_{mgra-crop}$ and sup-
 521 plementary Figure S16 reports the time series of different realizations of the N surplus for
 522 agricultural areas.

523 We combine the ten point sources and the 27 N surplus realizations to create 270 sets of
 524 N inputs. For each of them, we perform Monte-Carlo simulations from the same parameter
 525 sample of size 100,000 described in Section 4.1. This produces a total input-output sample
 526 of size 27,000,000. We then discard simulations that do not satisfy the soft rules defined in
 527 Section 4.1 to obtain the sample for the sensitivity analysis.

528 We apply the distribution-based PAWN sensitivity analysis method (Pianosi & Wa-
 529 gener, 2015) that evaluates the effect of the input factors on the entire output (here legacy
 530 stores) distribution. We estimate the PAWN sensitivity indices using the numerical approx-
 531 imation strategy introduced by Pianosi and Wagener (2018), which can be utilized for any
 532 generic input-output sample, and which is implemented in the Python version of the SAFE
 533 toolbox (Pianosi et al., 2015). With this numerical scheme, the range of variation of the
 534 i -th input factor is partitioned into a number n_i of equally probable “conditioning” intervals
 535 (denotes as $I_{i,k}$, $k=1, \dots, n_i$), each interval containing the same number of parameter sets.
 536 The PAWN method consists of the comparison between 1) the Cumulative Distribution
 537 Functions (CDFs) of the model output (denoted here as y) obtained by letting all input
 538 factors vary in their entire space of variability (i.e., unconditional CDF, denoted as $F_y(y)$)
 539 and 2) the CDF obtained by allowing all input factors to vary freely, but the i -th input x_i
 540 whose value is constrained to a specific conditioning interval (i.e., conditional CDF, denoted
 541 as $F_{y|x_i}(y|x_i)$). In PAWN, input sensitivity is quantified through the Kolmogorov-Smirnov
 542 statistic (KS, Kolmogorov, 1933; Smirnov, 1939), which is the maximum vertical distance,
 543 between unconditional and conditional CDFs. The PAWN sensitivity index for the i -th
 544 input factor, denoted as S_{PAWN}^i (-), aggregates the KS values calculated across all n_i con-
 545 ditioning intervals through a summary statistic, which is chosen as the median value in this

546 study, to eliminate the impact of outlier values:

$$547 \quad S_{PAWN}^i = Q_{50}^{x_i} KS(x_i) \quad (10)$$

548 where

$$549 \quad KS(x_i) = \max_y |F_y(y) - F_{y|x_i}(y|x_i)| \quad (11)$$

550 S_{PAWN}^i takes values between 0 and 1, and the higher its value the larger the impact
 551 of that input on the model output. For the ELEMeNT parameters, we adopt a number of
 552 conditioning intervals n_i equal to 10. For the N point sources, we calculate the conditional
 553 CDF for each of the ten realizations, and for the three N surplus parameters we compute
 554 the conditional CDF for each of their three selected values. We estimate the 95% confidence
 555 intervals of the PAWN sensitivity indices using 1000 bootstrap resamples, and we verify the
 556 convergence of the results given the sample size, following Sarrazin et al. (2016).

57 **5 Results**

58 **5.1 Parameter Estimation**

59 **5.1.1 Application of the Soft Rules**

560 The performance of the simulated in-stream N loading and concentration is compara-
 561 ble in terms of the metrics $RBIAS$ and STD_{err} (Figure 2a). However, in terms of ρ , the
 562 performance is noticeably better for the simulated N loading compared to the concentration
 563 for five subcatchments. For the three other subcatchments (outlet Hemelingen, Drakenburg
 564 and Wahnhausen), performance are more similar although higher values of ρ can be reached
 565 for the loading. In contrast to the concentration dynamics, the temporal fluctuations of
 566 the loading are strongly influenced by the discharge dynamics, which is an input to the
 567 ELEMeNT model. Importantly, we identify simulations that comply with each soft rule
 568 individually, as shown in the grey shaded areas in Figure 2a for rules 1-6 and in supplemen-
 569 tary Figure S17 for rule 7 (source zone N content). We also find that the threshold values
 570 on the performance metrics introduced in rules 1-6 result in values of the KGE higher than
 571 0.62 for the loading and 0.49 for the concentration in the behavioural simulation ensemble
 572 (grey shaded areas in right panels of Figure 2a). We verify that these KGE values are higher
 573 than the mean benchmark value of -0.41 (Knoben et al., 2019).

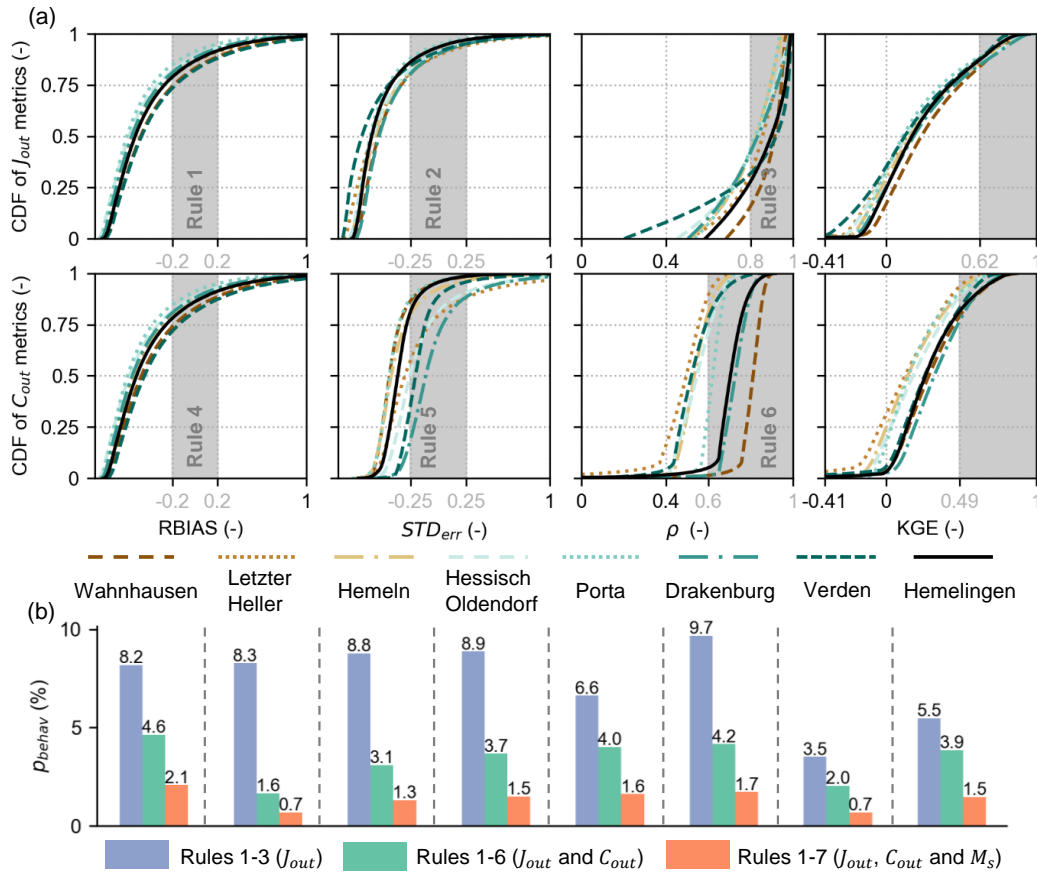


Figure 2. Application of the soft rules: (a) Cumulative Distribution Function (CDF) of the performance metrics for in-stream N loading (J_{out}) and concentration (C_{out}) in the initial simulation ensemble (100,000 realizations) and (b) percentage of realizations of the initial ensemble identified as behavioural (p_{behav}) by successive application of the soft rules based on the performance metrics for loading (J_{out} , rules 1-3), the performance metrics for concentration (C_{out} , rules 4-6), and the source zone N content (M_s , rule 7). The name of the eight subcatchments refer to both the legend of the lines of panel (a) and the bar graphs of panel (b). Panel (a) reports the three performance metrics used in the definition of rules 1-6 (relative bias $RBIAS$, variability error STD_{err} and Pearson correlation coefficient ρ) and the Kling-Gupta efficiency (KGE). The grey shaded areas and grey numbers on the x-axis indicate the behavioural ranges of the performance metrics used in the definition of rules 1-6. The ranges of the performance metrics shown (x-axis of plots in panel a) do not include the extreme values, which are shown in supplementary Figure S18.

574 From Figure 2b, we observe a reduction in the number of ELEMeNT realizations after
 575 application of the rules on the loading (rules 1-3), but also a further diminution after appli-
 576 cations of the rules on the concentration (rules 4-6) and on the source zone N content (rule
 577 7). This means that not only the loading, but also the concentration and the source zone
 578 N content have a value in constraining the simulations. In addition, the data on the source
 579 zone N content in 2009 (rule 7) allows reduction in the uncertainty in the total source zone
 580 N storage that is not constrained by the other rules (Figure S17). We obtain a number of
 581 behavioural simulations that varies between 676 for Letzter Heller and 2076 for Wahnhausen
 582 (supplementary Table S6). For further details on the reduction in the number of realiza-
 583 tions obtained when applying each of the seven rules individually, we refer to supplementary
 584 Figure S19.

585 ***5.1.2 Constraining of the Simulated In-stream Loading and Concentration***

586 From Figures 3-4, we observe that the precision of the simulated in-stream N loading
 587 and concentration is larger in the behavioural simulation ensemble compared to the uncon-
 588 strained ensemble, i.e., the red shaded areas are much narrower than the grey shaded areas.
 589 We also see that, for some years, the width of the 95% confidence interval (CI) of the simu-
 590 lation ensemble is reduced when applying the rules on the concentration and source zone N
 591 content (rules 4-7, red shaded areas) in addition to the rules on the loading (rules 1-3, blue
 592 shaded areas). However, the information on the source zone N content in 2009 (rule 7) does
 593 not further narrow down the uncertainty bounds, i.e., we do not observe green shaded ar-
 594 eas. Importantly, after applying the seven rules, the behavioural simulation ensembles (red
 595 shaded areas in Figures 3-4) capture a large number of observations. Specifically for most
 596 subcatchments, the simulation ensemble encompasses more than 90% of the observations,
 597 except for Verden for which it includes 57% of the observations.

598 Regarding loading (Figure 3), the temporal dynamics follow the discharge dynamics
 599 (discharge is reported in supplementary Figures S6-S13), and we see that the simulation
 600 ensembles match the observations very well. Regarding concentration (Figure 4), we ob-
 601 serve that the simulations are overall in agreement with the measurements. However, the
 602 median ensemble has difficulties in reproducing the observed concentration trend around
 603 the last ten years of the simulations (2005-2015), in particular at Hemeln, Porta, Verden
 604 and Hemelingen. While the measurements indicate a slight decrease in concentration, the
 605 latter is relatively stable in the simulations, which is consistent with the N input dynamics

606 over this time period (see Figure 1). Nonetheless, the simulation ensemble captures the ob-
 607 servations for all locations apart from Verden. We also notice that for Letzter Heller (panel
 608 b), concentration shows little temporal variations, while the N surplus trajectory presents
 609 a sharp decrease in 1990 (as shown in Figure 1).

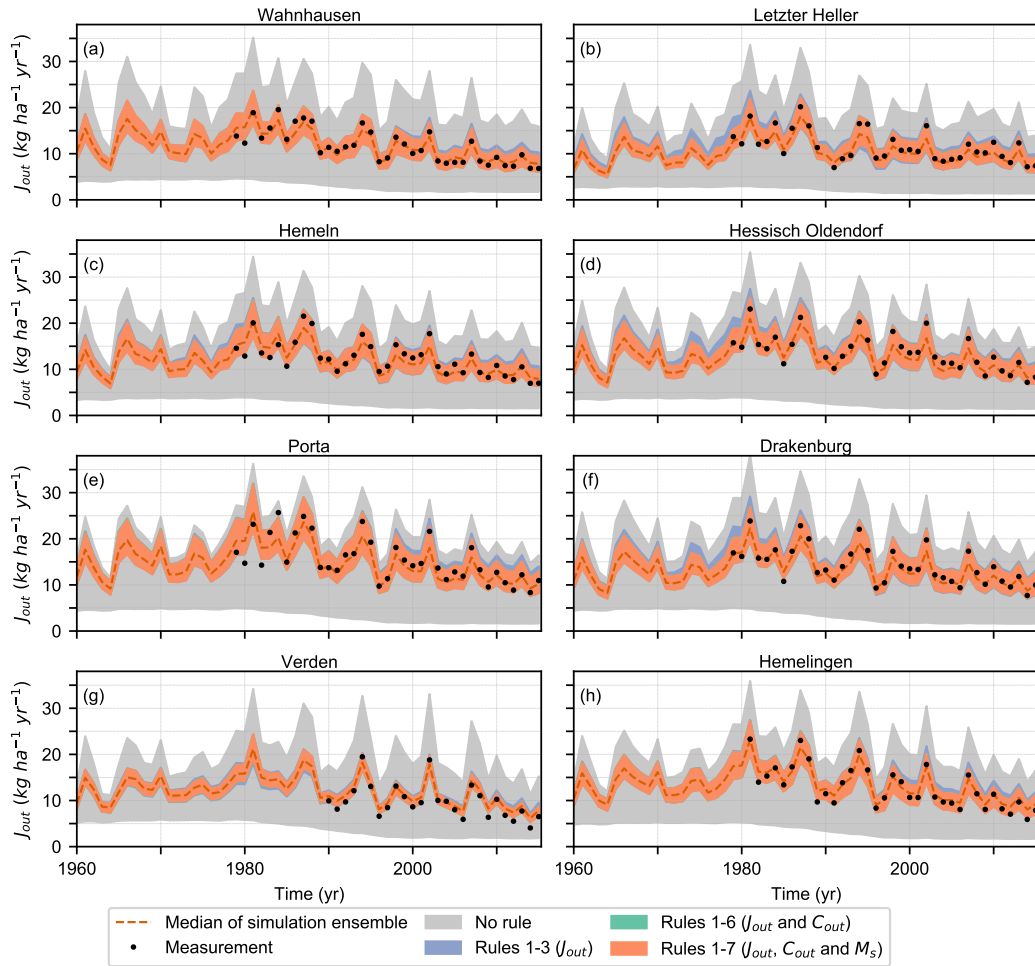


Figure 3. Simulated annual in-stream N- NO_3 loading (J_{out}) for the eight subcatchments. The dashed red lines represent the median of the behavioural simulation ensembles that satisfy all seven soft rules. The shaded areas represent the 95% CI of the simulation ensembles corresponding to four different levels of constraining.

610 **5.1.3 Constraining of the Parameter Distributions**

611 From Figure 5, we find that the differences between the prior (grey lines) and posterior
 612 (colored lines) CDFs of the parameters are very small for four parameters, namely the two

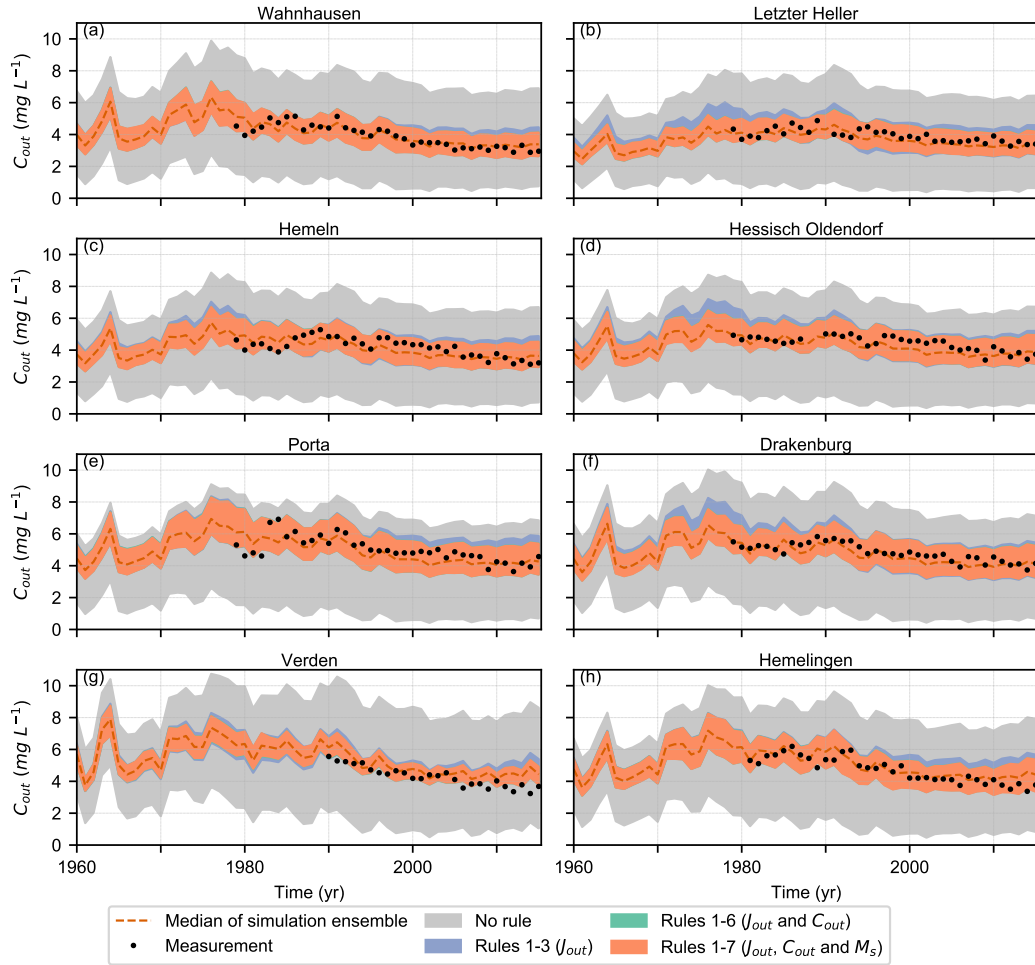


Figure 4. Simulated annual in-stream N- NO_3 concentration (C_{out}) for the eight subcatchments. The dashed red lines represent the median of the behavioural simulation ensembles that satisfy all seven soft rules. The shaded areas represent the 95% CI of the simulation ensembles corresponding to four different levels of constraining.

613 protection coefficients (h_c and h_{nc}), the mean annual water content in the source zone (V_s)
 614 and the fraction of in-stream N removal (R). Nonetheless, the median of the distribution
 615 changes by at least 20% for V_s for one subcatchment (increase of 25% for Letzter Heller)
 616 and for R for four subcatchments (decrease of 27% for Wahnhausen, 20% for Hemeln, 22%
 617 for Porta and 23% for Hemelingen). The other five parameters (M_{sorg}^{prist} , k_a , λ_s , λ_{sub} , and
 618 μ_{sub}) show appreciable (higher than 15%) reduction in their 95% CI. On average, these
 619 parameters exhibit a diminution in their CI of 59%, 10%, 37% 15% and 33%, respectively.
 620 The two denitrification rate constants (λ_s and λ_{sub}) and the mean travel time (μ_{sub}) take

621 values in the lower range of their prior distribution for most subcatchments, with median
 622 values in the range 0.28–0.34 yr^{-1} (prior: 0.55 yr^{-1}), 0.06–0.17 yr^{-1} (prior: 0.15 yr^{-1})
 623 and 8–19 yr (prior: 26 yr), respectively. The 95% CI of the travel time in the posterior
 624 distribution is reduced for the some subcatchments such as Hemelingen (95% CI: 2–24 yr),
 625 while it can still be rather large for some other subcatchments such as Drakenburg (95% CI:
 626 3–44 yr). The mineralization rate constant for organic active N (k_a) is unlikely to take values
 627 in the lower range of its prior distribution, as the lower bound of its 95% CI is in the range
 628 0.09–0.18 yr^{-1} (prior: 0.07 yr^{-1}). Details on the median and 95% CI of the parameter
 629 values are reported in supplementary Tables S7–S8. In addition, all three observational
 630 data used (loading, concentration and source zone N content) have value in constraining
 631 the distribution of at least one parameter, as shown in supplementary Figures S20–S27.
 632 In particular, the source zone N content observations in 2009 is the only data source that
 633 allows to constrain the source zone organic N stock under pristine conditions ($M_{s_{org}}^{prist}$).

634 We also calculate the behavioural values of the mean transfer times for the source
 635 zone organic N stores as the inverse of the respective mineralization rate constants. The
 636 mineralization rate constant for the protected pool is computed from Equation S24 and its
 637 CDFs can be visualized in supplementary Figure S28. We find that the mean transfer times
 638 for the protected store are much higher compared to the active store for all subcatchments.
 639 The median values (95% CI) of the mean transfer times are in the range 2000–2700 yr
 640 (1300–5400 yr) and 2.0–3.0 yr (1.4–11.3 yr) for the protected and active stores, respectively
 641 (more details in supplementary Table S9).

642 Interestingly, the parameter distributions for the upstream Letzter Heller subcatchment
 643 stands out, with particularly low median values of k_a , and high median values of μ_{sub}
 644 compared to the other subcatchments, including the Wahnhausen subcatchment which is
 645 neighbouring the Letzter Heller and which has similar land use and topography (Figure 1,
 646 Section 3.1). The results suggest that, compared to the other subcatchments, Letzter Heller
 647 may have a particularly high potential to accumulate organic active N in the source zone,
 648 due to the low mineralization rate for the active N pool (median value: 0.33 yr^{-1}), and
 649 dissolved mineral N in the subsurface, due to the large travel time (median value: 17 yr).

650 Overall, our results demonstrate that, for each of the eight subcatchments, multiple
 651 combinations of model parameter values lead to acceptable model performance. This equifi-
 652 nality can be partly explained by interactions between the model parameters, in particular

653 between the two denitrification rate constants in source zone and subsurface, between each
 654 of the denitrification rate constant and the mean travel time in the subsurface, between
 655 the denitrification rate constant in the subsurface and the fraction of in-stream removal
 656 and between the two protection coefficients (a detailed interaction analysis is presented in
 657 Table S10).

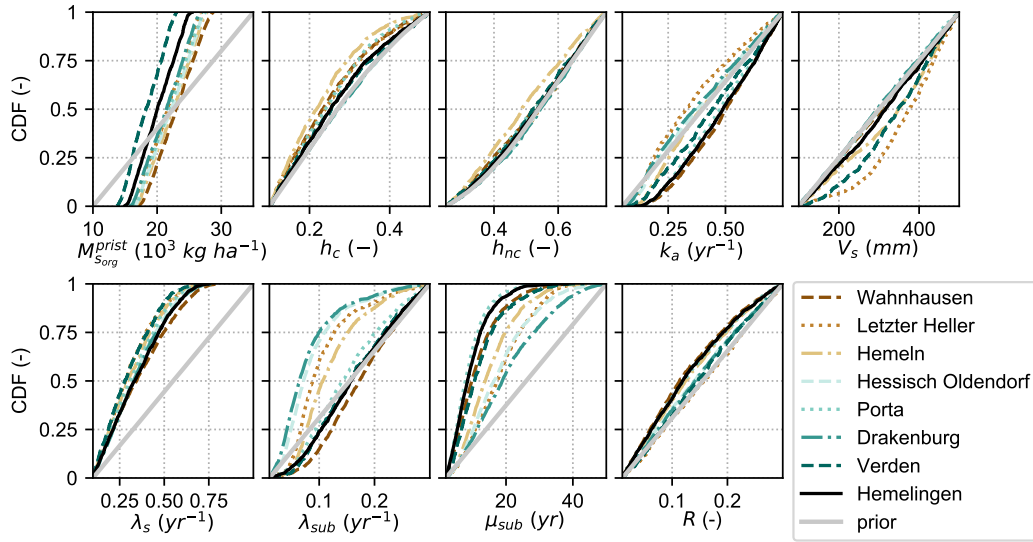


Figure 5. Cumulative distribution functions (CDFs) of the model parameters for the eight subcatchments. Colored lines refer to the behavioural CDFs, which are obtained after applications of the seven soft rules, and grey lines refer to the prior CDFs in the original sample of size 100,000. The prior CDFs are the same for all subcatchments.

658 5.2 Mass balance Over the Study Domain

659 5.2.1 Fate of the N Surplus

660 In this section, we examine the fate of the N surplus over the period 1960–2015 from the
 661 behavioural simulation ensemble (Figure 6, Table 2). Over the entire WRB (Hemelingen),
 662 the total denitrification in the source zone and subsurface ($J_{den_{tot}}$) amounts to 1888 kg ha^{-1}
 663 (median value), which corresponds to about 63% of the N surplus (95% CI: 49–74%). Around
 664 50% (median value) of the total denitrification occurs in the source zone, but the uncertainty
 665 in the partitioning of denitrification between source zone and subsurface is large (95% CI of
 666 the source zone contribution: 18–94%; supplementary Table S11).

667 The landscape export of N from catchment ($J_{out_{sub}}$) is equal to 537 kg ha^{-1} (median
 668 value), which represents 18% of the N surplus. As the initial source zone N storage in 1960
 669 is very large (median value: $17,487 \text{ kg ha}^{-1}$; 95% CI: $13,678\text{--}21,564 \text{ kg ha}^{-1}$), the change
 670 in the source zone N storage (ΔM_s , biogeochemical legacy) is relatively small with respect
 671 to this initial storage (median value: 2.5%; 95% CI: 1.2-5.1%; see details in supplementary
 672 Figure S30 and Table S12). Nevertheless, the change in the source zone storage amounts to
 673 448 kg ha^{-1} , (median value), which constitutes a high percentage of the N surplus (15%)
 674 similar to the stream export part. The 95% CI is however large for this component ($229\text{--}781$
 675 kg ha^{-1}) and is largely overlapping with the 95% CI of the stream export. The two last
 676 components per order of magnitude are the in-stream removal ($J_{rem_{sub}}$) and the change in
 677 the subsurface N storage (ΔM_{sub} , hydrologic legacy), which have median values equal to 72
 678 and 37 kg ha^{-1} respectively (which correspond to 2% and 1% of the N surplus respectively),
 679 and which have overlapping 95% CI. Therefore, the denitrification in the source zone and
 680 subsurface is an order of magnitude greater than the in-stream removal. Moreover, the N
 681 accumulation in the source zone is an order of magnitude higher than the N accumulation
 682 in the subsurface. Total legacy buildup in the WRB amounts to 491 kg ha^{-1} (95% CI:
 683 $264\text{--}820 \text{ kg ha}^{-1}$), which corresponds to around 16% of the N surplus.

684 We also observe that the simulated source zone N store is continuously building up
 685 in time over the period 1960–2015 (Figure 6a). In the subsurface, the dynamics of the N
 686 store is much more coupled to the dynamics of the N surplus (Figure 6b). We see that
 687 the N storage in the subsurface increases until the 1987 to reach a value of 61 kg ha^{-1}
 688 (median value), decreases by about as much as 40% between 1987 and 2010, and shows
 689 small fluctuations between 2010 and 2015.

690 For the different subcatchments, the relative importance of the different components of
 691 the N mass balance are similar (Table 2). In particular, denitrification $J_{den_{tot}}$ is always the
 692 largest outgoing N flux. The median change in source zone storage ΔM_s generally varies
 693 between 473 kg ha^{-1} (Hemeln) and 584 kg ha^{-1} (Drakenburg). An exception is the Verden
 694 subcatchment, which is mostly located in the lowland areas, and for which the median ΔM_s
 695 is smaller (326 kg ha^{-1}). The median change in subsurface storage ΔM_{sub} is smaller for
 696 Wahnhausen (17 kg ha^{-1}) and is larger for Letzter Heller (62 kg ha^{-1}), Hessisch Olden-
 697 dorf (62 kg ha^{-1}) and Drakenburg (78 kg ha^{-1}). The relatively large value of ΔM_{sub} for
 698 Letzter Heller compared to the other subcatchments is consistent with the parameter dis-
 699 tribution results presented in Section 5.1.3. We also observe that the (temporal) dynamics

700 of N buildup in the legacy stores of all subcatchments are similar to those of Hemelingen
701 (see supplementary Figures S29-S31). In particular, N levels in the subsurface peak around
702 the year 1990. Notably, the highest level of N accumulation in the subsurface across sub-
703 catchments and time is equal to 119 kg ha^{-1} (median value) and is reached for Drakenburg
704 in 1993 and Letzter Heller in 1987. However, the differences found between catchments are
705 not robust, since the 95% CI are largely overlapping between subcatchments.

706 We also examine the change in the different N stores of the source zone, i.e., the organic
707 protected, organic active, and inorganic N stores (details in supplementary Table S12). Most
708 of the N accumulation occurs in the protected pool (e.g. 94% for Hemelingen; 95% CI: 79–
709 98%). For Hemelingen, N buildup amounts to 448 kg ha^{-1} (95% CI: $229\text{--}781 \text{ kg ha}^{-1}$) in
710 the protected store, to 21 kg ha^{-1} (95% CI: $12\text{--}74 \text{ kg ha}^{-1}$) in the active store, and to 2
711 kg ha^{-1} (95% CI: $-5\text{--}16 \text{ kg ha}^{-1}$) in the inorganic store.

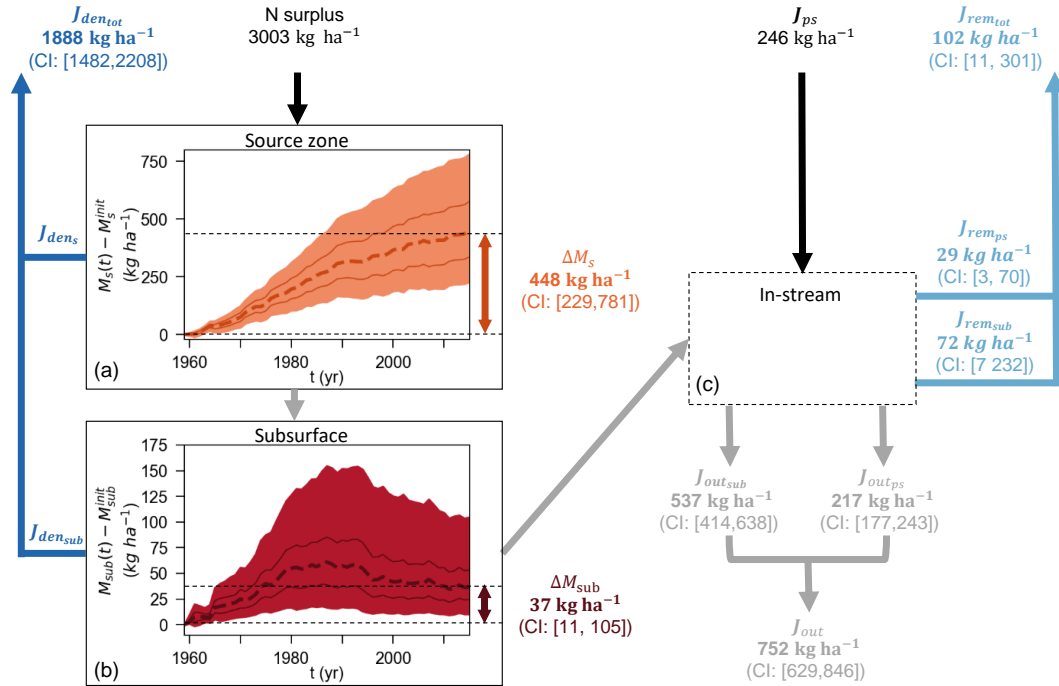


Figure 6. Cumulative values of the components of the N mass balance (inputs and simulated variables) for the WRB at Hemelingen for the period 1960–2015. For the simulated variables, the figure reports the median values and the 95% CI in the behavioural simulation ensemble. Panels (a–b) report the simulated cumulative change in N storage for the source zone (M_s) and the subsurface zone (M_{sub}) since 1960 as a function of time t (M_s^{init} and M_{sub}^{init} are the initial conditions in 1960 for the source zone and subsurface storage respectively). The shaded areas indicate the 95% CI, the solid lines the 25% and 75% quantiles and the dashed lines the median values. Panel (c) represents the in-stream compartment, where no accumulation of N occurs in ELEMEnT. Notations: J_{ps} is the point source; J_{out} is the simulated in-stream loading, which is the sum of the point source contribution ($J_{out_{ps}}$) and the subsurface contribution ($J_{out_{sub}}$); $J_{den_{tot}}$ is the total denitrification, which is the sum of the denitrification in the source zone (J_{den_s}) and in the subsurface ($J_{den_{sub}}$); $J_{rem_{tot}}$ is the in-stream removal, which is the sum of the removal of the point source contribution ($J_{rem_{ps}}$) and the subsurface contribution ($J_{rem_{sub}}$); ΔM_s is the change in the source zone storage which includes three N stores (organic protected, organic active, and inorganic N stores); ΔM_{sub} is the change in the subsurface storage.

Table 2. Components of the N Mass Balance in the Behavioural Simulation Ensemble for the Period 1960–2015

Variable	Wahn- hausen	Letzter Heller	Hemeln	Hessisch Olden- dorf	Porta	Draken- burg	Verden	Heme- lingen
	$(kg\ ha^{-1})$							
<i>Surplus</i>	3093	2917	3004	3041	3075	3179	2697	3003
$J_{out_{sub}}$	477 ⁶⁰⁴ ₃₆₁	461 ⁵⁸⁶ ₃₈₂	513 ⁶⁴⁵ ₄₀₄	550 ⁷⁰⁴ ₄₅₅	632 ⁸¹³ ₅₁₀	553 ⁷⁰⁶ ₄₄₄	446 ⁵⁰⁰ ₃₉₂	537 ⁶³⁸ ₄₁₄
$J_{den_{tot}}$	2001 ²³¹⁵ ₁₆₁₆	1805 ²⁰⁹⁶ ₁₄₇₃	1872 ²¹⁶⁹ ₁₅₀₁	1787 ²¹²⁴ ₁₄₁₂	1787 ²¹²⁸ ₁₄₀₃	1838 ²²¹⁴ ₁₄₃₆	1786 ²⁰⁸⁸ ₁₄₃₆	1888 ²²⁰⁸ ₁₄₈₂
$J_{rem_{sub}}$	62 ²¹⁴ ₇	88 ²¹² ₈	72 ²²⁴ ₇	91 ²⁴⁹ ₉	87 ²⁷⁶ ₈	91 ²⁵⁰ ₉	75 ¹⁹² ₈	72 ²³² ₇
ΔM_s	504 ⁸²⁸ ₂₉₀	480 ⁷⁶⁴ ₂₇₀	473 ⁷⁸⁶ ₂₈₃	526 ⁸⁰³ ₂₇₈	485 ⁸⁰⁷ ₂₈₃	584 ⁹¹¹ ₃₀₆	326 ⁶⁴² ₈₀	448 ⁷⁸¹ ₂₂₉
ΔM_{sub}	17 ⁵⁴ ₅	62 ¹³⁸ ₁₅	39 ¹⁰⁰ ₁₀	62 ¹⁶⁰ ₁₆	30 ⁹⁰ ₉	78 ²⁰⁶ ₁₇	44 ¹⁴² ₁₁	37 ¹⁰⁵ ₁₁
J_{ps}	214	144	183	180	226	226	274	246
$J_{out_{ps}}$	190 ²¹¹ ₁₅₃	121 ¹⁴¹ ₁₀₂	161 ¹⁸¹ ₁₃₁	154 ¹⁷⁶ ₁₂₇	199 ²²³ ₁₆₂	194 ²²² ₁₆₁	234 ²⁶⁹ ₁₉₄	217 ²⁴³ ₁₇₆
$J_{rem_{ps}}$	24 ⁶¹ ₃	23 ⁴² ₃	23 ⁵² ₃	25 ⁵² ₃	27 ⁶⁴ ₃	32 ⁶⁶ ₄	40 ⁸⁰ ₅	29 ⁷⁰ ₃
	$(\% \text{ N input})$							
<i>Surplus</i>	100	100	100	100	100	100	100	100
$J_{out_{sub}}$	15 ²⁰ ₁₂	16 ²⁰ ₁₃	17 ²¹ ₁₃	18 ²³ ₁₅	21 ²⁶ ₁₇	17 ²² ₁₄	17 ¹⁹ ₁₅	18 ²¹ ₁₄
$J_{den_{tot}}$	65 ⁷⁵ ₅₂	62 ⁷² ₅₁	62 ⁷² ₅₀	59 ⁷⁰ ₄₆	58 ⁶⁹ ₄₆	58 ⁷⁰ ₄₅	66 ⁷⁷ ₅₃	63 ⁷⁴ ₄₉
$J_{rem_{sub}}$	2 ⁷ ₀	3 ⁷ ₀	2 ⁷ ₀	3 ⁸ ₀	3 ⁹ ₀	3 ⁸ ₀	3 ⁷ ₀	2 ⁸ ₀
ΔM_s	16 ²⁷ ₉	16 ²⁶ ₉	16 ²⁶ ₉	17 ²⁶ ₉	16 ²⁶ ₉	18 ²⁹ ₁₀	12 ²⁴ ₃	15 ²⁶ ₈
ΔM_{sub}	1 ² ₀	2 ⁵ ₁	1 ³ ₀	2 ⁵ ₁	1 ³ ₀	2 ⁶ ₁	2 ⁵ ₀	1 ³ ₀
J_{ps}	100	100	100	100	100	100	100	100
$J_{out_{ps}}$	89 ⁹⁹ ₇₁	84 ⁹⁸ ₇₁	88 ⁹⁹ ₇₁	86 ⁹⁸ ₇₁	88 ⁹⁹ ₇₂	86 ⁹⁸ ₇₁	85 ⁹⁸ ₇₁	88 ⁹⁹ ₇₂
$J_{rem_{ps}}$	11 ²⁹ ₁	16 ²⁹ ₂	12 ²⁹ ₁	14 ²⁹ ₂	12 ²⁸ ₁	14 ²⁹ ₂	15 ²⁹ ₂	12 ²⁸ ₁

Notes: The table reports the fate for the N surplus: the stream export ($J_{out_{sub}}$), the total denitrification in source zone and subsurface ($J_{den_{tot}}$), the in-stream removal ($J_{rem_{sub}}$), the change in the source zone storage (ΔM_s) which includes three N stores (organic protected, organic active, and inorganic N stores), and the change in the subsurface storage (ΔM_{sub}). It also reports the fate for the N point sources (J_{ps}): the stream export ($J_{out_{ps}}$), and the in-stream removal ($J_{rem_{ps}}$). For simulated variables, numbers indicate the median, and lower bound (lb) and upper bound (ub) of the 95% CI in the behavioural simulation ensemble: $median_{lb}^{ub}$.

5.2.2 Contribution of the N Point Sources to the In-stream N Loading

We investigate the contribution of the in-stream N loading originating from N point sources ($J_{out_{ps}}$) to the total in-stream loading (J_{out}) over the period 1960–2015. For Hemelingen, we find that the N point sources are an important flux that amounts to 217 $kg\ ha^{-1}$, and that accounts for 28.7% of the total in-stream N loading (Table 2 and supplementary Table S13). For all subcatchments, the N points sources contribution to the total in-stream N loading is between 20% and 29%, apart from Verden for which it is as high as 34.4% (median values, as reported in supplementary Table S13). We note that the 95% CI on the point sources contribution is rather large, as e.g. for Hemelingen it is 22.6–35.6%. This can be partly explained by the large uncertainty in the in-stream N removal (Table 2), since behavioural estimates of R can span over its entire prior range (0.01–0.3) for all subcatchments (Figure 5). For the last ten years of the simulation period (2006–2015), i.e., when the point sources is at its lowest level, N point sources still contribute to between 14% and 20% of the total in-stream N loading (95% CI: 10–26%) across all subcatchments (supplementary Table S13).

To understand the relative role of point and diffuse (N surplus) sources on the resulting temporal trend of the total in-stream N concentration, we perform a piecewise linear trend analysis for each individual component of the concentration over different time periods for Hemelingen. The analysis is based on the median of the behavioural simulation ensemble (total concentration is represented by a dashed red line in Figure 4-h). For the period 1970–1990, with respect to the total concentration, we find no statistically significant trend (significance level: 0.01) and a very small slope of the regression line ($s_{lin}=-0.01\ mg\ L^{-1}\ yr^{-1}$), which is explained by the contrasting trends in the diffuse sources contribution (negative slope of the regression line $s_{lin}=-0.08\ mg\ L^{-1}\ yr^{-1}$) and point sources contributions (positive slope of the regression line $s_{lin}=0.07\ mg\ L^{-1}\ yr^{-1}$). For the period 1990–2000, the total concentration shows a marked decreasing trend ($s_{lin}=-0.16\ mg\ L^{-1}\ yr^{-1}$). Over the same time period, the point sources show a stronger decline ($s_{lin}=-0.1\ mg\ L^{-1}\ yr^{-1}$) compared to the diffuse sources ($s_{lin}=-0.05\ mg\ L^{-1}\ yr^{-1}$). During the last time period 2000–2015, the concentration trends are either non-significant for the total concentration and the point sources contribution, or small for the diffuse sources contribution ($s_{lin}=-0.02\ mg\ L^{-1}\ yr^{-1}$). The concentration time series used for this trend analysis and the regression lines are reported in supplementary Figure S32.

5.3 Uncertainty and Sensitivity of the Simulated N Legacies

Section 5.2.1 mostly focuses on examining the median values of the simulated N legacies. However the uncertainty is large (Table 2), due to the limited information available to constrain these legacies. The soft rules hardly affect the distribution of the simulated change in source zone storage (ΔM_s , top panel of Figure 7). The width of the 95% CI in the behavioural ensemble is about equal to the median value, apart from Verden for which it is 1.7 time higher (red boxplots). Regarding the subsurface, the soft rules can have a contrasting effect on the simulated change in storage (ΔM_{sub} , bottom panel of Figure 7), as they can reduce but also exacerbate the uncertainty. Values that are outliers, i.e., beyond the 95% CI of the grey boxplots, in the unconstrained ensemble can be identified as behavioural and be included in the constrained 95% CI (colored boxplots). The width of the 95% CI for ΔM_{sub} is between two to three times higher than the median value.

Here, we investigate the factors that explain this residual uncertainty in the legacy N stores by assessing the sensitivity of the simulated N legacies to the ELEMeNT parameters, the N point sources and the N surplus in the constrained simulation ensemble obtained after application of the soft rules, for Hemelingen (see method in Section 4.2). For each of the 270 combinations of N surplus and N point sources, we identify between 531 and 2146 behavioural simulations (details in supplementary Table S14 and Figures S33–35). This results in a total sample of the model input-output of size 362,985 to perform the PAWN sensitivity analysis. We observe that the bootstrap confidence intervals of the estimated sensitivity indices are narrow and exhibit little overlap among the different inputs (Figure 8). Therefore, the sample size is sufficient to infer a robust ranking of the input factors according to their relative importance.

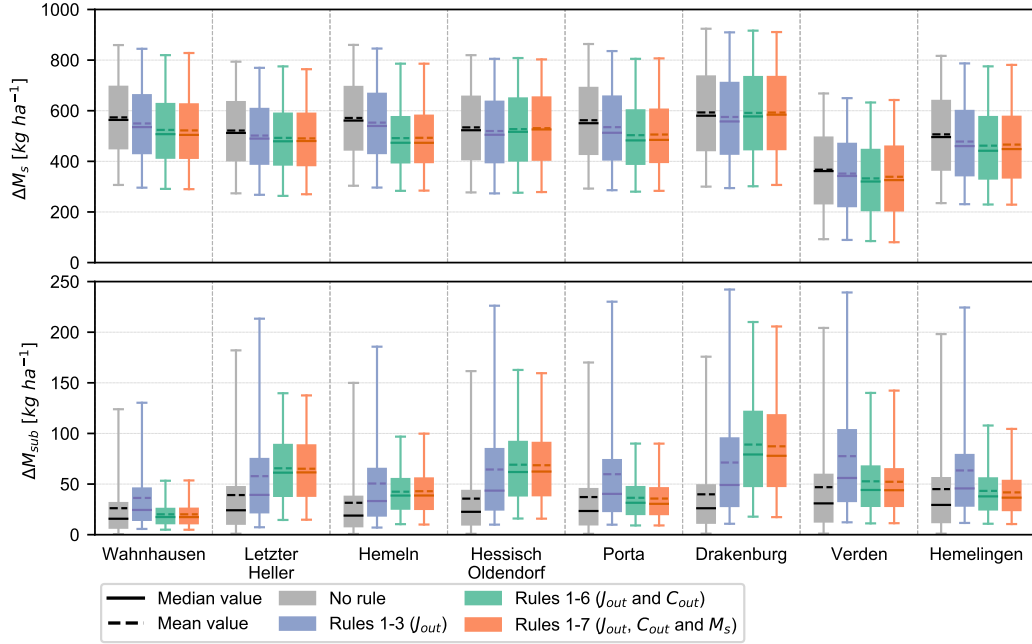


Figure 7. Statistics of the simulated N legacies for the period 1960–2015 (change in source zone N storage – ΔM_s , and change in subsurface N storage – ΔM_{sub}) obtained for different levels of constraining. The source zone N storage includes the three N storages (organic protected, organic active, and inorganic N stores). The boxplots report the median (solid line), mean (dashed line), 2.5%, 25%, 75% and 97.5% quantiles of the simulation ensembles.

767 From Figure 8 we observe that the N point sources (PS) and two parameters used
 768 to generate the N surplus realizations, namely the ratio of the N surplus for agricultural
 769 permanent grassland to the N surplus for cropland ($r_{mgra-crop}$) and the ratio of the agricul-
 770 tural N surplus in 1850 to the value in 1950 (r_{warm}) have very small sensitivity indices and
 771 are the least sensitive inputs for all four output variables considered. This means that the
 772 uncertainties in the ELEMent parameters and in the value of the total N surplus (multi-
 773 plier parameter $f_{surplus}$) have a much larger impact on the behavioural values of the legacy
 774 stores than the uncertainties in PS , $r_{mgra-crop}$, and r_{warm} .

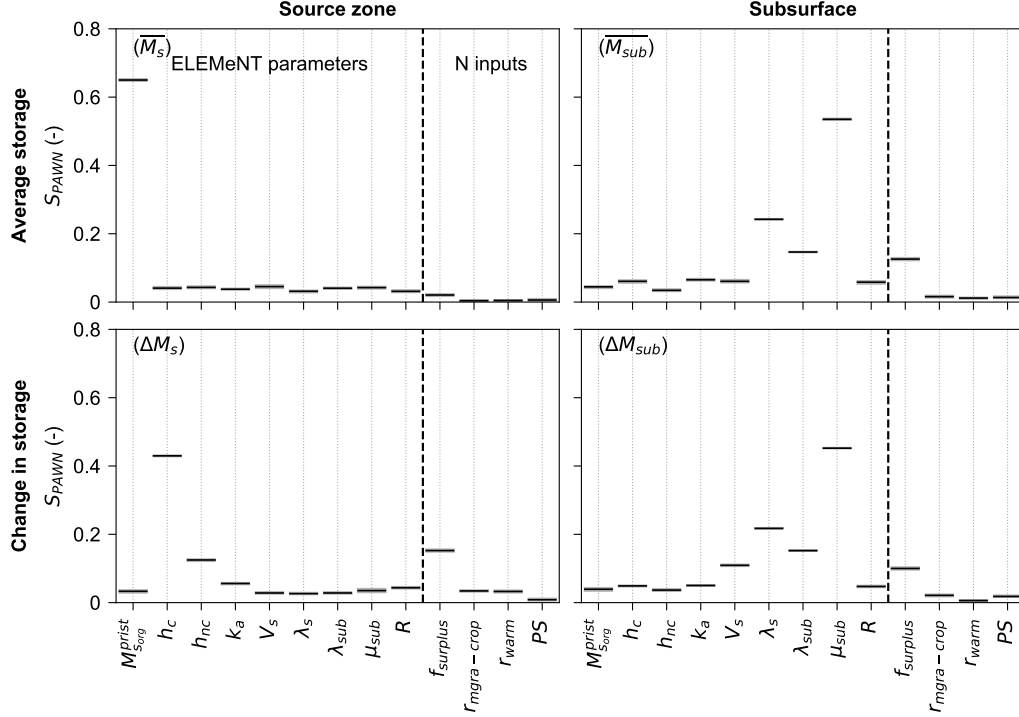


Figure 8. PAWN sensitivity indices S_{PAWN} of the nine ELEMeNT parameters, the three parameters introduced to generate alternative N surplus realizations ($f_{surplus}$, $r_{mgra-crop}$, and r_{warm}), and the N point sources realization (PS), for the WRB at Hemelingen. Sensitivity indices are reported with respect to four model outputs evaluated over the period 1960–2015, namely the average source zone N storage \overline{M}_s , the average subsurface N storage \overline{M}_{sub} , the cumulative change in source zone N storage ΔM_s , and the cumulative change in subsurface N storage ΔM_{sub} . The source zone N storage includes the three N storages (organic protected, organic active, and inorganic N stores). The horizontal black lines indicate the bootstrap mean value of the sensitivity indices, while the grey boxes represent the 95% bootstrap confidence intervals. The bootstrap confidence intervals are very small (the grey boxes are very narrow), since the size of the sample used to calculate the PAWN indices is very large.

775 For the source zone, the sensitivity analysis results with respect to the average N
 776 storage ($\overline{M_s}$) and the change in N storage (ΔM_s) differ. The protection coefficient for
 777 cultivated land (h_c) is largely responsible for the uncertainty in ΔM_s , followed by the N
 778 surplus multiplier ($f_{surplus}$) and the protection coefficient for non-cultivated land (h_{nc})
 779 whose sensitivity indices have similar magnitude. In contrast, the source zone organic N
 780 stock under pristine conditions ($M_{s_{org}}^{prist}$) is by far the most influential parameter for $\overline{M_s}$. For
 781 the subsurface zone, unlike the source zone, results are similar for the two statistics analyzed
 782 (the average N storage $\overline{M_{sub}}$ and the change in N storage ΔM_{sub}), and a larger number of
 783 input factors are influential. Specifically, the mean travel time in the subsurface (μ_{sub}) is the
 784 most influential input, followed in decreasing order of importance by the denitrification rate
 785 constants in the source zone (λ_s) and in the subsurface (λ_{sub}), and the N surplus multiplier
 786 ($f_{surplus}$). In addition the mean annual water content in the source zone (V_s) has a stronger
 787 impact on the change in the subsurface N storage than on the average storage. The value
 788 of the sensitivity index of V_s with respect to the change in subsurface storage is similar to
 789 the sensitivity index of $f_{surplus}$.

790 The importance of the three N surplus parameters and the N point sources may be
 791 higher than suggested by the PAWN analysis because the parameter estimation may re-
 792 sult in different posterior parameter distributions when using different N input realizations.
 793 Therefore, the application of the soft rules may compensate for the uncertainties in the N
 794 inputs. This effect is particularly visible for the N surplus multiplier, which has some impact
 795 on the distributions of the mean travel time and the denitrification rate constants (supple-
 796 mentary Figure S38), but it is much less pronounced for the other N inputs parameters
 797 (supplementary Figure S36–37).

798 We further examine the robustness of the PAWN analysis by estimating the sensitivity
 799 indices using other summary statistics (mean and maximum values) than the median value,
 800 to aggregate the KS values across the conditioning intervals in Equation 10. As shown in
 801 Figures S39–S40, the results show a similar order of importance among all inputs (model
 802 parameters and N input realizations) as shown in Figure 8. We however note that, when
 803 using the maximum KS, the mineralization rate constant for the active store (k_a) has a
 804 sensitivity index of the same magnitude as $f_{surplus}$ with respect to the average subsurface
 805 storage. From supplementary Figures S41–S44 that report the conditional and unconditional
 806 CDFs used for the calculation of the PAWN indices, we see that k_a has a higher impact in
 807 the lower 10% of its range (values lower than 0.25 yr^{-1}) on the average subsurface storage.

6 Discussion

6.1 Performance of the Simulated In-stream N Loading and Concentration

The ELEMeNT model is able to produce simulations that are consistent with observations of in-stream N loading and concentration (i.e., that show satisfactory values for each of the three components of the KGE), and with the source zone N content in 2009 for the different study catchments (Figures 2-4). While previous studies using the ELEMeNT model (Chang et al., 2021; J. Liu et al., 2021; Van Meter et al., 2017) focused on simulating the in-stream N loading, here we also examine the concentration, which is more difficult to simulate than the loading (Husic et al., 2019). As seen in our results, the loading dynamics are predominantly determined by the discharge dynamics, while the concentration dynamics may be the results of more complex processes. It is important to assess both N loading and concentration to characterize the in-stream water quality status, as N loading affects the status in downstream receiving water, while concentration describes the local water quality status (Hirsch et al., 2010).

Although, our simulations are overall in good agreement with the observations, we observe a discrepancy between the median simulated N concentration and the measured values for the later years (2005–2015). This is particularly visible at Verden, where the concentration observations are at the lower end or lower than the behavioural simulation ensemble for this time period. First, this mismatch between simulated and observed concentration could be due to changes in the characteristics of the landscape (such as e.g. the density of tile drains as observed in J. Liu et al. (2021)), that could require temporally varying parameter values. However, no information is available to us to substantiate that such changes have occurred. Second, another possible cause for the discrepancy between observed and simulated concentration could be the uncertainty in the N input data (N surplus and N point sources). In particular, in Germany, data on application of mineral fertilizer exist at the national level only. For lower administrative levels, data refer to the sale of mineral fertilizer and are therefore strongly linked to the location of the fertilizer companies, rather than the actual amount of fertilizer application. Therefore, subjective choices have to be made to disaggregate the fertilizer application amounts to finer spatial units (Häußermann et al., 2020; Behrendt et al., 2003). Fertilizer application is an important component of the N surplus and changes have been implemented after 2007 due to a new ordinance that limits fertilizer use (DüV, 2007). This could contribute to the uncertainty in our in-stream

840 simulations. In Section 6.3.2, we further elaborate on the need for a better estimation of
841 the uncertainty in the N surplus for an improved characterization of not only the in-stream
842 variables, but also the N legacy stores.

843 **6.2 N Mass Balance in the WRB and its Implications for Water and Land** 844 **Management**

845 ***6.2.1 Denitrification in the Terrestrial Compartments***

846 Our results (Figure 6 and Table 2) indicate that denitrification in the terrestrial system
847 (source zone and subsurface) is the largest sink for the N surplus in the WRB for the period
848 1960–2015. This is consistent with previous modelling studies of N legacies performed in
849 North America, namely Ilampooranan et al. (2019) using the SWAT-LAG model, and J. Liu
850 et al. (2021) and Van Meter et al. (2017) using the ELEMeNT model. However, we find
851 that denitrification is much higher for the WRB, in that it is likely to be higher than 50%
852 for the eight subcatchments, while it is found to be less than 50% in the three previous
853 studies. Such a high amount of denitrification in the WRB could have adverse consequences
854 on the atmosphere and the climate, because it can potentially release nitrous oxide (N_2O).
855 Yet, N_2O can be further reduced into harmless dinitrogen N_2 in presence of favourable
856 environmental conditions in the soil and subsurface (Betlach & Tiedje, 1981; Bergsma et
857 al., 2002; Robertson & Groffman, 2015; Rivett et al., 2008). The results of ongoing efforts,
858 such as the “Global N_2O Model Intercomparison Project” (Tian et al., 2018), will be key
859 to better understand and quantify the processes involved in N_2O emissions and the impact
860 of denitrification on the atmosphere.

861 ***6.2.2 Accumulation of N Legacies***

862 In this study, we explicitly quantify the N legacies in the WRB over the period 1960–
863 2015 (Figure 6 and Table 2). Previous N modelling studies in the WRB are either based
864 on a simple regression model that does not account for N storages in the terrestrial system
865 (GREEN model; Grizzetti et al., 2008), or on a modelling framework that represents the
866 residence time of N in the groundwater, but that does not consider source zone N storage
867 nor assesses the long-term accumulation of N in the subsurface (Heidecke et al., 2015; Hirt
868 et al., 2012; Kreins et al., 2010). We find that the N accumulation in the source zone, which
869 amounts to 15% of the N surplus (95% CI: 8–26%), is an order of magnitude higher than

870 the N accumulation in the subsurface, which is equal to less than 3% of the N surplus. The
871 magnitude of the simulated N accumulation in the source zone and the subsurface is similar
872 across subcatchments. Groundwater nitrate concentration is found to be higher than the
873 regulatory threshold of 11.3 mg L^{-1} in some measuring points in the WRB, in particular
874 in Lower Saxony (NLWKN, 2019), while background levels are typically very low. This
875 supports our result that N has been building up in the subsurface. However, no information
876 is available on the N accumulation in the source zone to corroborate our findings. In previous
877 studies of N legacies, the relative value of biogeochemical and hydrologic N legacies is highly
878 variable. Whereas the N buildup in the subsurface store is also found to be lower than the
879 buildup in the source zone in the Grand river basin (J. Liu et al., 2021), a subcatchment of
880 the Iowa-Cedar basin (Ilampooranan et al., 2019) and the Mississippi river basin (Van Meter
881 et al., 2017), the opposite result is reported for the Susquehanna river basin (Van Meter et
882 al., 2017). The magnitude of hydrologic N legacies in J. Liu et al. (2021) is similar to our
883 study (around 4% of the N surplus), while it reaches 14% in Ilampooranan et al. (2019).

884 Although the N accumulation in the subsurface represents a small fraction of the N
885 surplus in the WRB, this N store is composed of reactive and dissolved N forms, which
886 can be easily accessed and mobilized. Thus, they are of immediate relevance for the water
887 quality status. Since the mean travel time in the subsurface is found to be equal to 8 yr
888 (95% CI: 2–24 yr), the subsurface N storage is likely to impact the stream N concentration
889 over the coming years. In the source zone, the accumulated N could be a threat for future
890 water N levels as well, depending on how fast it can mineralize. Findings of previous studies
891 suggest that applied N fertilizer can slowly leach over decades following their application
892 (Haag & Kaupenjohann, 2001; Sebilo et al., 2013). Our results indicate that most of the N
893 accumulation occurs in the organic protected N pool (median value for Hemelingen: 94%,
894 Table S12), whose transfer time is in the order of magnitude of a few millennia (Table S9).
895 The N buildup is much smaller in the active pool that has a transfer time of a few years to a
896 decade. The long transfer times of N stored in the source zone, which can be made possible
897 through the protection of N into organic matter (Six et al., 2002), may partly explain why it
898 is difficult to lower the N concentrations to acceptable values in the WRB and, more broadly,
899 in regions with long history of high N inputs, as described e.g. in Grimvall et al. (2000)
900 and Vero et al. (2018). Source zone N storage could also be a potential resource for crop
901 growth, allowing satisfaction of the crop N requirements with lower amounts of fertilizer
902 application, as proposed by Dupas et al. (2020) and J. Liu et al. (2021). In particular, while

903 it is widely accepted that crops can use mineral N compounds present in the soil, they may
904 also take up organic N forms, but this process is still not well understood (Näsholm et al.,
905 2009; Farzadfar et al., 2021). Therefore, the fate of the N stored in the source zone has
906 large uncertainties and depends on the ability of the plants to access it and on its potential
907 to mineralize to yield more available N forms.

908 Regarding the temporal dynamics, the permanent buildup in the source zone found for
909 the WRB is consistent with most of the previous N legacy studies (Ilampooranan et al.,
910 2019; J. Liu et al., 2021; Van Meter et al., 2016). The WRB shows a large decrease in
911 the subsurface N store during the period 1990–2010, that can be explained by the concur-
912 rent reduction in the N surplus. Hydrologic N legacies permit to sustain higher in-stream
913 concentration levels over this time period. This is particularly visible for the Letzter Heller
914 subcatchment, which has undergone a large and sudden decrease in the N surplus after 1990,
915 while in-stream N concentration remains relatively stable. This result for the subsurface N
916 legacy differs from earlier legacy studies over the Mississippi and Susquehanna river basins
917 and the subcatchment of the Iowa-Cedar river basins, where the subsurface N store is con-
918 tinuously building up in time (Ilampooranan et al., 2019; Van Meter et al., 2016). Given the
919 importance of the N legacies for land and water management and in particular to achieve
920 the target of 2.8 mg L^{-1} for in-stream concentration in the WRB (OGewV, 2016), better
921 characterization and reduction of the uncertainties in the simulated N legacies is crucial, as
922 further discussed in Section 6.3.

923 ***6.2.3 Importance of the N Point Sources***

924 We find that N point sources from wastewater represent an important fraction of the
925 in-stream nitrate loading in the WRB (Figure 6, Tables 2 and S13). Point sources N loads
926 comprise 28.7% (95% CI: 22.6–35.6%) of the stream N load for the period 1960–2015. The
927 contribution is smaller for the later period (2006–2015), where point sources have a lower
928 magnitude due widespread connection to wastewater treatment plants and high efficiency
929 of treatment. Grizzetti et al. (2008) find that point sources account for 31% of the stream
930 N-NO₃ loading over the period 1995–2002 for the WRB at Hemelingen. This is higher
931 than our uncertainty estimates for this time period (95% CI: 13–23%, Table S13), which
932 could be explained by the differences in the model structure used in Grizzetti et al. (2008)
933 (regression based GREEN model) and in the N point sources inputs. In our study, the N
934 point sources are constrained by recent observations of N loading from wastewater treatment

935 plants (Section 3.2.4), while Grizzetti et al. (2008) do not make use of observational data.
936 Moreover, the temporal variations in the N point sources have a large effect on the trend
937 of the total in-stream N concentration during the period 1970–2000 (Figure S32). The
938 decrease in the N point sources during the 1970s and 1980s counteracts the increase in the
939 contribution of the N diffuse sources (N surplus) to the in-stream N concentration, resulting
940 in no overall trend in the total concentration. The marked decrease in the total concentration
941 in the 1990s is also largely dominated by the decrease in the point sources. While the N
942 diffuse sources are the largest contributor in magnitude to the in-stream concentration, their
943 temporal signal can be smoothed through biogeochemical transformations and transport in
944 the source zone and subsurface (Figure S32). In contrast, changes in the N point sources have
945 an immediate impact on the in-stream concentration and can therefore strongly influence
946 its trend.

947 Some past N modelling studies covering a large range of catchments across Germany
948 and France have not accounted for N point sources (Dupas et al., 2020; Ehrhardt et al.,
949 2021). Based on our simulation results, we recommend the consideration of N point sources
950 and their temporal variations in future N modeling analyses over the WRB.

951 **6.3 Towards Reducing the Uncertainty and Equifinality in the Simulations** 952 **of a N Model**

953 *6.3.1 Value of the Soft Rules to Constrain the Model Uncertainties*

954 In this study, we utilize three different sets of observational data (in-stream N loading
955 and concentration and source zone N content) to estimate the model parameters, using a
956 portfolio of soft rules to constrain the model results. We show that, beyond in-stream N
957 loading, in-stream concentration and source zone N content have a value in reducing the
958 number of behavioural simulations and in constraining the parameter distributions, thus
959 reducing the equifinality (Figure 2b, Figure 5). Specifically, the in-stream N loading and
960 concentration data affect the simulated in-stream loading and concentration (Figures 3,4)
961 and the simulated change in the subsurface storage (Figure 7). The source zone N content
962 is the only data that allows to constrain the magnitude of the total simulated N storage
963 (Figure S17), but it has no appreciable impact on the different components of the mass
964 balance (Figures 3,4,7). Importantly, the soft rules do not constrain the change in the
965 source zone N store (Figure 7).

966 Only few previous N modelling studies analyzed the equifinality by performing a de-
967 tailed investigation of the parameter space, including Husic et al. (2019) and Rankinen et
968 al. (2006). Due to the different model structures used in these studies, our parameter esti-
969 mation results cannot be directly compared to these studies. Yet, we note that Rankinen
970 et al. (2006) reveals a strong interplay between terrestrial and in-stream model processes in
971 a subcatchments of the Simojokiriver basin in Finland. This is consistent with our results,
972 as we could barely constrain the in-stream N removal parameter (R).

973 Despite the equifinality we can constrain the range of a few parameters, including the
974 mean travel time in the subsurface μ_{sub} , which we determine to be equal to 8 yr (95%
975 CI: 2–24 yr) at Hemelingen (Table S7). Koeniger et al. (2008) reports values of the mean
976 groundwater travel time in the range 8-93 yr (37 yr for total flow) for Hemelingen, based on
977 long-term tritium isotope data in combination with simulations from a hydrologic model.
978 Hirt et al. (2012) found a value of the mean travel time in the groundwater of 25 yr. Ehrhardt
979 et al. (2021) established that the overall mode travel time for total flow are in the range 0-20
980 yr for different subcatchments of the WRB and in particular in the range 0-10 yr for most
981 subcatchments. Therefore previous studies cover a large spectrum of travel time values,
982 which includes our estimates. The results of the study of Hirt et al. (2012) are also, as
983 expected, on the higher end of our uncertainty estimates. This can be because Hirt et al.
984 (2012) explicitly account for quicker flow paths (tile drainage) in their modelling framework,
985 while in ELEMeNT all flow paths to the stream are lumped in the subsurface compartment.

986 The soft rules only allow to reduce part of the equifinality, as some parameter distri-
987 butions could be hardly constrained (Figure 5) and the uncertainty in the model internal
988 components remains large (Figure 7). For example, it would be relevant to determine the
989 amount of denitrification occurring in the source zone and the subsurface, because deni-
990 trification in the subsurface can involve the irreversible degradation of substances, such as
991 pyrite, which is not sustainable (Wendland et al., 2009; Wriedt & Rode, 2006). Such quan-
992 tification is however not possible due to equifinality (Figure 5, supplementary Table S11)
993 and therefore this topic deserves further investigations. In addition, establishing a robust
994 ranking of importance of the N legacy buildup between subcatchments would be desirable
995 to target management efforts to legacy hotspots (J. Liu et al., 2021). However, the residual
996 uncertainty in the simulated N legacies is still large (Figure 7) and the confidence intervals of
997 the distributions of the N buildup obtained for the different subcatchments are overlapping.

998 This equifinality can be due to parameter interactions (Table S10) or to the fact that some
999 model parameters are not influential with respect to the metrics used in the soft rules.

1000 **6.3.2 Strategies to Further Reduce the Uncertainty and Equifinality**

1001 To tackle this issue of uncertainty and equifinality, we perform a sensitivity analysis to
1002 investigate the factors that are responsible for the residual uncertainty in the simulated N
1003 legacy stores and that should be the focus of future efforts for uncertainty reduction (Fig-
1004 ure 8). We apply the PAWN method, which does not rely on any assumption regarding the
1005 model input-output relationship, to the constrained input-output sample. The studies of
1006 Van Meter et al. (2017) and J. Liu et al. (2021) assess the sensitivity of the median source
1007 zone N store simulated with the ELEMeNT model. Although the method adopted in these
1008 two studies is linear regression and the sensitivity analysis is carried out based on the uncon-
1009 strained sample before calibration, their results are comparable to our study. We observe
1010 that the most influential factor is by far the source zone organic N stock under pristine
1011 conditions ($M_{s_{org}}^{prist}$) in both our study and in J. Liu et al. (2021), and the mineralization
1012 rate constant for the organic protected pool, which is related to $M_{s_{org}}^{prist}$ (Equation S24)
1013 in Van Meter et al. (2017). We further note that Van Meter et al. (2017) and J. Liu et
1014 al. (2021) examine the sensitivity of the cumulative in-stream N loading and find, similar
1015 to our results for the average subsurface N store, that the mean travel time and the two
1016 denitrification rate constants in the source zone and the subsurface are the three most in-
1017 influential parameters. This similarity between the sensitivity of the in-stream N loading and
1018 the subsurface N store can be explained by the structure of the ELEMeNT model which
1019 lumps all flow paths to the stream into the subsurface store.

1020 Our sensitivity analysis (Figure 8) reveals that the protection coefficient for cultivated
1021 land is mostly responsible for the residual uncertainty in the simulated accumulation in
1022 the source zone N store. This parameter could scarcely be constrained by the soft rules
1023 (Figure 5). The protection coefficient is a conceptual parameter that partitions the N
1024 surplus between the organic active and protected N stores, and therefore it can hardly
1025 be inferred through field measurements. A possible solution could be to further refine
1026 and constrain the representation of the protection mechanism in the source zone using
1027 information gained from simulation experiments carried out with more complex models,
1028 that focus on the soil processes and that can include a large number of soil N pools, such as
1029 the DAISY (Hansen et al., 1991) or the CANDY model (Franko et al., 1995) (a review of soil

1030 organic matter models is provided in Campbell & Paustian, 2015). Regarding the buildup of
1031 the subsurface N store, three interacting parameters mostly contribute to the uncertainty,
1032 namely the mean travel time in the subsurface, which is also the most influential factor,
1033 and the two denitrification rate constants. In this regard, tracer studies, and in particular
1034 the combination of tritium concentration and helium isotope measurements, can help to
1035 characterize the travel time (Sültenfuß et al., 2009), as well as the modelling of conservative
1036 solutes, such as chloride, in combination with nitrate (Kaandorp et al., 2021). In addition,
1037 Eschenbach et al. (2018) propose a method to characterize denitrification in the groundwater,
1038 based on the measurement of the N_2/Ar ratio. Such techniques provide promising avenues
1039 for constraining denitrification fluxes and thereby possibly reducing the uncertainty in the
1040 simulated N legacies.

1041 Regarding the magnitude of the total N surplus, we characterize the uncertainty of
1042 this input data by using a time-invariant multiplier coefficient and we explore a variation
1043 of $\pm 20\%$ with respect to the baseline N surplus data. N surplus datasets for Germany
1044 do not provide uncertainty intervals, as uncertainty estimation is currently not a common
1045 practice in N surplus construction (X. Zhang et al., 2021). An improved assessment of this
1046 uncertainty in future studies seem necessary, since, on the one hand, our results show that
1047 the uncertainty in the N surplus has an impact (1) on the simulated N legacies (Figure 8),
1048 although this impact is smaller than the ELEMENNT parameters that we discussed previously
1049 in this section, (2) on the posterior distribution of the model parameters (Figure S38), and
1050 (3) possibly on the simulated in-stream concentration trend over the period 2005-2015 (as
1051 discussed in Section 6.1). On the other hand, X. Zhang et al. (2021) found large discrepancies
1052 in different components of the N surplus for agricultural areas between different global
1053 datasets, which suggests that the actual uncertainties in the N surplus can be large.

1054 We recognize that, in this study, the uncertainties on the different components of the
1055 N mass balance, including the simulated N legacy buildup, could be underestimated. In
1056 fact, we examine the uncertainties in the N surplus using exploratory coefficients that may
1057 not reflect the actual uncertainties in the N surplus. We also do not investigate the model
1058 structural uncertainties. To further address the modelling uncertainties and equifinality,
1059 future studies need to reveal not only the uncertainties in the model parameter values, but
1060 also in the data used as input or to constrain the simulations, and in the model structures,
1061 as elaborated below.

1062 First, regarding the parameters values, the definition of the parameter distributions
1063 and ranges can affect the parameter estimation results, because they can greatly impact the
1064 sensitivity of the metrics used for calibration (e.g. the bias, variability error or correlation
1065 used in this study) to the model parameters (a discussion on the impact of the parameter
1066 ranges on sensitivity analysis results is provided e.g. in Pianosi et al., 2016). To address
1067 this issue, in this study, we define the ranges through a careful literature review (Table 1).

1068 Second, with respect to the data uncertainties, in this study we focus on the N inputs
1069 and the soil N data (used in the soft rules). Including uncertainty on soil N data is crucial
1070 especially, if the objective is to detect a change in storage when data are provided for
1071 different years. Given the large size of the total N storage (Table S12), the change in
1072 storage may be within the observation uncertainties. In our study, we consider that other
1073 data uncertainties are smaller. In fact, the annual stream discharge data is the combination
1074 of observations, and evaluated and bias-corrected model simulations (Section 3.2.5). In
1075 contrast, no observational data of N surplus exist to test the plausibility of the N surplus
1076 estimates. We also consider that the in-stream N concentration data has a high quality,
1077 since they come from 14-day average measurements (Section 3.2.6). However, uncertainty
1078 should be examined when data have a lower quality, in particular when using low-frequency
1079 in-stream concentration observations combined with weighted regressions on time, discharge
1080 and season (WRTDS, Hirsch et al., 2010). In this respect, a bootstrap approach could be
1081 envisaged (Hirsch et al., 2015).

1082 Third, a modelling approach allowing for systematic exploration of different modelling
1083 alternatives could be developed, similar to the Structure for Unifying Multiple Modeling
1084 Alternatives (SUMMA, Clark et al., 2015a, 2015b) that allow testing of alternative model
1085 formulations for a range of different hydrological and thermodynamic processes. Specifically,
1086 in the source zone, worth of further investigation are the representation of the processes of
1087 immobilization of N into organic matter and of N saturation, which are poorly character-
1088 ized (Bingham & Cotrufo, 2016; Yansheng et al., 2020). In the subsurface, further mixing
1089 schemes beyond complete mixing/random sampling could be examined using StorAge Se-
1090 lection (SAS) functions, as implemented e.g. in Nguyen et al. (2021).

1091 To help identification of plausible model structures and parameters values, our study call
1092 for the long-term monitoring of N content in the soil and along the subsurface (unsaturated
1093 zone and groundwater) profile. Current N data in the subsurface are typically provided

1094 at a unique depth below the water table at each measuring site, e.g. in the European
1095 Waterbase dataset (EEA, 2021) or in the dataset provided by the German state of Lower
1096 Saxony (NLWKN, 2022). These data do not allow straightforward quantification of the
1097 subsurface N storage, since nitrate concentration can vary greatly with the depth to the
1098 water table (MacDonald et al., 2017; Rudolph et al., 1998) and large amounts of N could
1099 also be stored in the unsaturated zone (Ascott et al., 2017). Regarding the soil part, future
1100 modelling studies could make use of the data on soil mineral N content that will likely
1101 become available, in particular in Germany where the 2017 fertilizer ordinance (DüV, 2017)
1102 prescribes the investigation of soil mineral N prior to fertilizer application.

1103 Yet, due to the scale mismatch between point scale measurements of soil and subsurface
1104 N content and the modelling resolutions, the incorporation of these data into the modelling
1105 exercise requires the use of smart techniques and appropriate model structures that are com-
1106 mensurate with the measurements (Peters-Lidard et al., 2017). Moving towards the use of
1107 spatially distributed water quality models (X. Yang et al., 2018; Nguyen et al., 2021) may be
1108 a way forward for integrating local scale measurements into the modelling framework. Such
1109 models should be however combined with smart parameterization techniques, such as the
1110 Multiscale Parameter Regionalization (MPR, Kumar et al., 2013; Samaniego et al., 2010),
1111 which allows for seamless simulations at multiple scales and facilitates the incorporation of
1112 finer level information (Rakovec et al., 2016; Samaniego et al., 2017).

1113 **7 Conclusions**

1114 The objectives of this study were to 1) characterize the uncertainties in the long-term
1115 fate of the N inputs to the landscape, simulated with a parsimonious catchment-scale N
1116 model (ELEM_eNT), 2) determine the value of different (observational) data to constrain
1117 the simulation results with emphasis on the simulated N legacies, and 3) gain further under-
1118 standing of the magnitude and dynamics of the N legacies to determine their relevance for
1119 water and land management. To do so, we establish the ELEM_eNT model in eight nested
1120 sub-catchments of the WRB, and simulate the fate of N and the dynamics of the legacy
1121 stores over the last six decades (1960–2015).

1122 We introduce a multicriteria parameter estimation strategy based on soft rules, that
1123 imposes acceptability limits to the model performance in reproducing the in-stream N load-
1124 ing and concentration, and the source zone N content in 2009. We demonstrate that this

1125 procedure allows to reduce the equifinality. In particular, the in-stream data allow to con-
1126 strain the simulated in-stream N loading and concentration and the change in the subsurface
1127 N storage, while the source zone N content data reduce the uncertainty in the simulated
1128 total source zone N storage. All sources of information also have value in constraining the
1129 parameter distributions. However, despite the parsimonious structure of the ELEMeNT
1130 model, the uncertainties in the mass balance components remain substantial after using all
1131 available information to constrain the simulations. This is due to equifinality, and more
1132 specifically to interactions between the model parameters, e.g. between the travel time in
1133 the subsurface and the denitrification rate constants. Our sensitivity analysis reveals crucial
1134 information on model functioning by identifying key model parameters, such as the protec-
1135 tion coefficient for cultivated land, the travel time in the subsurface and the denitrification
1136 rate constants in the source zone and the subsurface, that are largely responsible for the
1137 residual uncertainty in the simulated N legacies. The N surplus input could also be an im-
1138 portant source of uncertainty. Its uncertainty estimates should be better assessed in future
1139 works to refine the exploratory multiplier coefficient approach used in this study.

1140 Given our modelling assumptions and the data we used, our simulation results suggest
1141 a relative importance of the different constituents of the N mass balance in the WRB over
1142 the period 1960–2015. Denitrification is found to be the largest sink for the N surplus and
1143 is likely to be higher than 50%, followed by the in-stream N export and source zone N
1144 accumulation – both with similar magnitude (median value: 15–18%), while subsurface N
1145 accumulation and in-stream N removal appear to be the smaller components (lower than
1146 4%). Total accumulation in legacies stores in the WRB amounts to around 491 kg ha^{-1}
1147 (95% CI: $264\text{--}820 \text{ kg ha}^{-1}$). Although the buildup of the subsurface N store represents a
1148 small proportion of the N surplus, it constitutes an immediate threat for the water quality
1149 status, since it includes mobile N forms. Furthermore, our analysis reveals N point sources
1150 as one of the important contributors to the in-stream N levels (median value: 28.7% over
1151 the period 1960–2015); and therefore we recommend that more attention should be given
1152 to this component to properly analyze N dynamics in future modeling studies.

1153 Overall, we recognize that our simulation results have large uncertainties. Our study
1154 calls for a thorough consideration of equifinality in catchment water quality modelling, for
1155 a better characterization of the model internal components, such as the biogeochemical and
1156 hydrologic N legacies. Although knowledge about N legacies is crucial to reach the water
1157 quality goals and improve the ecological status of water bodies, this topic deserves more

1158 attention. In particular, modelling of N legacies is fraught with a myriad of uncertainties
1159 arising from different sources, including not only the model parameter values and input data
1160 that are examined in this study, but also the model structures and sparse measurements
1161 (e.g. low-frequency in-stream concentration observations). To this end, we believe that
1162 sensitivity analysis can be a promising tool for tackling the uncertainty and equifinality. In
1163 fact, it allows identification and pinpointing of the model input factors that are responsible
1164 for the uncertainty and that should be the focus of future efforts for uncertainty reduction.
1165 Importantly, spatially lumped or semi-distributed model structures may restrict the amount
1166 of observational data that can be incorporated into the modelling framework, because of
1167 the incommensurability between the data, and the model parameter and corresponding
1168 simulations. Therefore, future efforts towards reducing the equifinality should focus on both
1169 collecting further data, and improving the model representations (e.g. parameterization and
1170 structures).

1171 **Open Research**

1172 The land use, N surplus, N point sources and mHM simulated discharge data, as
1173 well as the ELEMeNT simulated N output as available at [https://www.hydroshare.org/
1174 resource/8779a09b9f204172931a641dd27d00c4/](https://www.hydroshare.org/resource/8779a09b9f204172931a641dd27d00c4/). The underlying data used in this study
1175 were downloaded from: <https://datenbank.fgg-weser.de/weserdatenbank> (in-stream
1176 nitrate concentration and river discharge data, FGG Weser, 2021); [http://www.bafg.de/
1177 GRDC](http://www.bafg.de/GRDC) (river discharge data Global Runoff Data Centre, 2021); [https://dataportaal.pbl
1178 .nl/downloads/HYDE/](https://dataportaal.pbl.nl/downloads/HYDE/) (History Database of the Global Environment – HYDE, Klein Gold-
1179 ewijk et al., 2017); <https://esgf-node.llnl.gov/> (atmospheric N deposition data); [https://
1180 land.copernicus.eu/pan-european/corine-land-cover](https://land.copernicus.eu/pan-european/corine-land-cover) (Corine Land Cover, EEA, 2019a);
1181 [https://esdac.jrc.ec.europa.eu/content/topsoil-physical-properties-europe-based
1182 -lucas-topsoil-data](https://esdac.jrc.ec.europa.eu/content/topsoil-physical-properties-europe-based-lucas-topsoil-data) (topsoil bulk density based on the Land Use and Cover Area frame
1183 statistical Survey – LUCAS data, Ballabio et al., 2016); [https://esdac.jrc.ec.europa
1184 .eu/content/chemical-properties-european-scale-based-lucas-topsoil-data](https://esdac.jrc.ec.europa.eu/content/chemical-properties-european-scale-based-lucas-topsoil-data) (soil N
1185 content based on LUCAS data, Ballabio et al., 2019); [http://www.fao.org/faostat/
1186 en/#data/FBSH](http://www.fao.org/faostat/en/#data/FBSH) and <http://www.fao.org/faostat/en/#data/FBS> (protein supply data,
1187 FAO, 2021a, 2021b); [http://appsso.eurostat.ec.europa.eu/nui/show.do?lang=en&dataset=
1188 env\ww\con](http://appsso.eurostat.ec.europa.eu/nui/show.do?lang=en&dataset=env\ww\con) and <https://db.nomics.world/Eurostat/env\wwcon\r2> (population con-
1189 nection to sewer and wastewater treatment, Eurostat, 2016, 2021).

1190 **Acknowledgments**

1191 Support to FS was provided by the Reduced Complexity Models project co-funded by the
 1192 Helmholtz Association. FS, RK, MW and SA acknowledge the Advanced Earth Modelling
 1193 Capacity (ESM) project funded by the Helmholtz Association. We thank Martin Bach
 1194 for providing the N surplus data for agricultural areas. We thank Oldrich Rakovec for
 1195 providing the long-term mHM simulations. We thank two anonymous referees for their
 1196 useful suggestions that allowed us to improve the quality of this paper.

1197 **References**

- 1198 Arle, J., Blondzik, K., Claussen, U., Duffek, A., Grimm, S., Hilliges, F., ... Wolter, R.
 1199 (2017). *Waters in Germany: Status and assessment German environment*. Dessau-
 1200 Roßlau, Germany: German Environment Agency.
- 1201 Ascott, M. J., Gooddy, D. C., Wang, L., Stuart, M. E., Lewis, M. A., Ward, R. S., &
 1202 Binley, A. M. (2017). Global patterns of nitrate storage in the vadose zone. *Nature*
 1203 *Communications*, 8, 1416. doi: 10.1038/s41467-017-01321-w
- 1204 Bach, M., Breuer, L., Frede, H., Huisman, J., Otte, A., & Waldhardt, R. (2006). Accu-
 1205 racy and congruency of three different digital land-use maps. *Landscape and Urban*
 1206 *Planning*, 78(4), 289–299. doi: 10.1016/j.landurbplan.2005.09.004
- 1207 Bach, M., & Frede, H.-G. (1998). Agricultural nitrogen, phosphorus and potassium bal-
 1208 ances in Germany — Methodology and trends 1970 to 1995. *Zeitschrift für Pflanzen-*
 1209 *ernährung und Bodenkunde*, 161(4), 385–393. doi: 10.1002/jpln.1998.3581610406
- 1210 Ballabio, C., Lugato, E., Fernández-Ugalde, O., Orgiazzi, A., Jones, A., Borrelli, P., ...
 1211 Panagos, P. (2019). Mapping LUCAS topsoil chemical properties at European scale
 1212 using Gaussian process regression. *Geoderma*, 355, 113912. doi: 10.1016/j.geoderma
 1213 .2019.113912
- 1214 Ballabio, C., Panagos, P., & Monatanarella, L. (2016). Mapping topsoil physical properties
 1215 at European scale using the LUCAS database. *Geoderma*, 261, 110–123. doi: 10.1016/
 1216 j.geoderma.2015.07.006
- 1217 Basu, N. B., Rao, P. S. C., Thompson, S. E., Loukinova, N. V., Donner, S. D., Ye, S., &
 1218 Sivapalan, M. (2011). Spatiotemporal averaging of in-stream solute removal dynamics.
 1219 *Water Resources Research*, 47(10), W00J06. doi: 10.1029/2010WR010196
- 1220 Batjes, N. (1996). Total carbon and nitrogen in the soils of the world. *European Journal of*
 1221 *Soil Science*, 47(2), 151–163. doi: 10.1111/j.1365-2389.1996.tb01386.x

- 1222 Behrendt, H., Bach, M., Kunkel, R., Opitz, D., Pagenkopf, W.-G., Scholz, G., &
1223 Wendland, F. (2003). *Nutrient Emissions into River Basins of Germany on*
1224 *the Basis of a Harmonized Procedure (Research report 299 22 285)*. Berlin,
1225 Germany: German Federal Environment Agency (Umweltbundesamt). Retrieved
1226 from [https://www.umweltbundesamt.de/en/publikationen/nutrient-emissions-](https://www.umweltbundesamt.de/en/publikationen/nutrient-emissions-into-river-basins-of-germany-on)
1227 [into-river-basins-of-germany-on](https://www.umweltbundesamt.de/en/publikationen/nutrient-emissions-into-river-basins-of-germany-on) (last access: 07 November 2021)
- 1228 Behrendt, H., Huber, P., Kornmilch, M., Opitz, D., Schmoll, O., Scholz, G., ... Schweikart,
1229 U. (2000). *Nutrient emissions into River Basins of Germany (Research report 296*
1230 *25 515)*. Berlin, Germany: German Federal Environment Agency (Umweltbun-
1231 desamt). Retrieved from [https://www.umweltbundesamt.de/en/publikationen/](https://www.umweltbundesamt.de/en/publikationen/nutrient-emissions-into-river-basins-of-germany)
1232 [nutrient-emissions-into-river-basins-of-germany](https://www.umweltbundesamt.de/en/publikationen/nutrient-emissions-into-river-basins-of-germany) (last access: 07 November
1233 2021)
- 1234 Benettin, P., Rinaldo, A., & Botter, G. (2015). Tracking residence times in hydrological
1235 systems: Forward and backward formulations. *Hydrological Processes*, *29*(25), 5203–
1236 5213. doi: 10.1002/hyp.10513
- 1237 Bergsma, T. T., Robertson, G. P., & Ostrom, N. E. (2002). Influence of soil moisture and
1238 land use history on denitrification end-products. *Journal of Environmental Quality*,
1239 *31*(3), 711–717. doi: 10.2134/jeq2002.7110
- 1240 Betlach, M. R., & Tiedje, J. M. (1981). Kinetic explanation for accumulation of nitrite, nitric
1241 oxide, and nitrous oxide during bacterial denitrification. *Applied and environmental*
1242 *microbiology*, *42*(6), 1074–1084. doi: 10.1128/AEM.42.6.1074-1084.1981
- 1243 Beven, K. (2006). A manifesto for the equifinality thesis. *Journal of Hydrology*, *320*(1-2),
1244 18–36. doi: 10.1016/j.jhydrol.2005.07.007
- 1245 Bingham, A. H., & Cotrufo, M. F. (2016). Organic nitrogen storage in mineral soil: Im-
1246 plications for policy and management. *Science of The Total Environment*, *551-552*,
1247 116–126. doi: 10.1016/j.scitotenv.2016.02.020
- 1248 Blankenau, K., Olf, H.-W., & Kuhlmann, H. (2001). Immobilization of fertilizer nitrogen
1249 and consequences for nitrogen fertilization of cereals. In W. J. Horst et al. (Ed.), *Plant*
1250 *Nutrition. Developments in Plant and Soil Sciences* (Vol. 92, pp. 796–797). Dordrecht:
1251 Springer. doi: 10.1007/0-306-47624-X_387
- 1252 BMEL. (2014). *Der Wald in Deutschland: Ausgewählte Ergebnisse der dritten*
1253 *Bundeswaldinventur*. Berlin, Germany: Bundesministerium für Ernährung und
1254 Landwirtschaft. Retrieved from <https://www.bmel.de/SharedDocs/Downloads/DE/>

- 1255 [Broschueren/bundeswaldinventur3.pdf?__blob=publicationFile&v=3](#) (last ac-
1256 cess: 25 January 2022)
- 1257 Botter, G., Bertuzzo, E., & Rinaldo, A. (2010). Transport in the hydrologic response:
1258 Travel time distributions, soil moisture dynamics, and the old water paradox. *Water*
1259 *Resources Research*, *46*(3), W03514. doi: 10.1029/2009WR008371
- 1260 Büttner, O. (2020). *DE-WWTP - data collection of wastewater treatment plants*
1261 *of Germany (status 2015, metadata)*. HydroShare [data set]. doi: 10.4211/hs
1262 .712c1df62aca4ef29688242eeab7940c
- 1263 Byrnes, D. K., Van Meter, K. J., & Basu, N. B. (2020). Long-Term shifts in U.S. nitrogen
1264 sources and sinks revealed by the new TREND-nitrogen data set (1930–2017). *Global*
1265 *Biogeochemical Cycles*, *34*(9), e2020GB006626. doi: 10.1029/2020GB006626
- 1266 Campbell, E. E., & Paustian, K. (2015). Current developments in soil organic matter
1267 modeling and the expansion of model applications: a review. *Environmental Research*
1268 *Letters*, *10*(12), 123004. doi: 10.1088/1748-9326/10/12/123004
- 1269 Castellano, M. J., Kaye, J. P., Lin, H., & Schmidt, J. P. (2012). Linking carbon saturation
1270 concepts to nitrogen saturation and retention. *Ecosystems*, *15*, 175–187. doi: 10
1271 .1007/s10021-011-9501-3
- 1272 Chang, S. Y., Zhang, Q., Byrnes, D. K., Basu, N. B., & Meter, K. J. V. (2021). Chesapeake
1273 legacies: the importance of legacy nitrogen to improving Chesapeake Bay water qual-
1274 ity. *Environmental Research Letters*, *16*(8), 085002. doi: 10.1088/1748-9326/ac0d7b
- 1275 Chen, D., Hu, M., & Dahlgren, R. A. (2014). A dynamic watershed model for determining
1276 the effects of transient storage on nitrogen export to rivers. *Water Resources Research*,
1277 *50*(10), 7714–7730. doi: 10.1002/2014WR015852
- 1278 Chen, D., Shen, H., Hu, M., Wang, J., Zhang, Y., & Dahlgren, R. A. (2018). Chapter
1279 Five - Legacy Nutrient Dynamics at the Watershed Scale: Principles, Modeling, and
1280 Implications. In D. L. Sparks (Ed.), *Advances in agronomy* (Vol. 149, pp. 237–313).
1281 Academic Press. doi: 10.1016/bs.agron.2018.01.005
- 1282 Choi, H. T., & Beven, K. (2007). Multi-period and multi-criteria model conditioning to
1283 reduce prediction uncertainty in an application of TOPMODEL within the GLUE
1284 framework. *Journal of Hydrology*, *332*(3-4), 316–336. doi: 10.1016/j.jhydrol.2006.07
1285 .012
- 1286 Clark, M. P., Nijssen, B., Lundquist, J. D., Kavetski, D., Rupp, D. E., Woods, R. A.,
1287 ... Rasmussen, R. M. (2015a). A unified approach for process-based hydrologic

- 1288 modeling: 1. modeling concept. *Water Resources Research*, 51(4), 2498–2514. doi:
1289 10.1002/2015WR017198
- 1290 Clark, M. P., Nijssen, B., Lundquist, J. D., Kavetski, D., Rupp, D. E., Woods, R. A., ...
1291 Marks, D. G. (2015b). A unified approach for process-based hydrologic modeling: 2.
1292 model implementation and case studies. *Water Resources Research*, 51(4), 2515–2542.
1293 doi: 10.1002/2015WR017200
- 1294 Cleveland, C. C., Townsend, A. R., Schimel, D. S., Fisher, H., Howarth, R. W., Hedin,
1295 L. O., ... Wasson, M. F. (1999). Global patterns of terrestrial biological nitrogen
1296 (n₂) fixation in natural ecosystems. *Global Biogeochemical Cycles*, 13(2), 623–645.
1297 doi: 10.1029/1999GB900014
- 1298 Damania, R., Desbureaux, S., Rodella, A.-S., Russ, J., & Zaveri, E. (2019). *Quality un-*
1299 *known: The invisible water crisis*. Washington, DC, USA: The World Bank. doi:
1300 10.1596/978-1-4648-1459-4
- 1301 Dehaspe, J., Sarrazin, F., Kumar, R., Fleckenstein, J. H., & Musolff, A. (2021). Bending of
1302 the concentration discharge relationship can inform about in-stream nitrate removal.
1303 *Hydrology and Earth System Sciences*, 25(12), 6437–6463. doi: 10.5194/hess-25-6437
1304 -2021
- 1305 Digizeitschriften. (2021). *Statistisches Jahrbuch*. Retrieved from [http://www](http://www.digizeitschriften.de/dms/toc/?PID=PPN635628112)
1306 [.digizeitschriften.de/dms/toc/?PID=PPN635628112](http://www.digizeitschriften.de/dms/toc/?PID=PPN635628112) (last access: 07 November
1307 2021)
- 1308 Dupas, R., Ehrhardt, S., Musolff, A., Fovet, O., & Durand, P. (2020). Long-term nitrogen
1309 retention and transit time distribution in agricultural catchments in western France.
1310 *Environmental Research Letters*, 15(11), 115011. doi: 10.1088/1748-9326/abbe47
- 1311 DüV. (2007). *Düngeverordnung vom 27. Februar 2007 (BGBl. I S. 221)*. Retrieved from
1312 https://www.umwelt-online.de/recht/lebensmt/dvo_ges.htm (last access: 28
1313 January 2022)
- 1314 DüV. (2017). *Düngeverordnung vom 26. Mai 2017 (BGBl. I S. 1305)*. Retrieved from
1315 http://www.gesetze-im-internet.de/d_v_2017/D%C3%BCV.pdf (last access: 28
1316 January 2022)
- 1317 EEA. (2015). *Waterbase-UWWTD version 1*. European Environmental Agency
1318 (EEA) [data set]. Retrieved from [https://www.eea.europa.eu/ds_resolveuid/](https://www.eea.europa.eu/ds_resolveuid/8396aa5079544dab9d8b8966237a9f3b)
1319 [8396aa5079544dab9d8b8966237a9f3b](https://www.eea.europa.eu/ds_resolveuid/8396aa5079544dab9d8b8966237a9f3b)
- 1320 EEA. (2018). *European waters: Assessment of status and pressures 2018* (No. European

- 1321 Environment Agency (EEA) report 7/2018). Luxembourg, Luxembourg: Publications
1322 Office of the European Union. doi: 10.2800/303664
- 1323 EEA. (2019a). *Corine Land Cover Version 20, Release date: 14-06-2019*. European Envi-
1324 ronment Agency (EEA) under the framework of the Copernicus Land Monitoring
1325 Service [data set]. Retrieved from [https://land.copernicus.eu/pan-european/
1326 corine-land-cover](https://land.copernicus.eu/pan-european/corine-land-cover) (last access: 07 November 2021)
- 1327 EEA. (2019b). *Nutrient enrichment and eutrophication in Europe's seas: Moving towards
1328 a healthy marine environment* (No. European Environment Agency (EEA) report
1329 14/2019). Luxembourg, Luxembourg: Publications Office of the European Union.
1330 doi: 10.2800/092643
- 1331 EEA. (2021). *Waterbase - Water Quality ICM*. European Environmental Agency
1332 (EEA) [data set]. Retrieved from [https://www.eea.europa.eu/ds_resolveuid/
1333 91fb02dc13cd485c81e8bbd048b5af8d](https://www.eea.europa.eu/ds_resolveuid/91fb02dc13cd485c81e8bbd048b5af8d) (last access: 28 January 2021)
- 1334 Ehrhardt, S., Ebeling, P., Dupas, R., Kumar, R., Fleckenstein, J. H., & Musolff, A.
1335 (2021). Nitrate transport and retention in Western European catchments are shaped
1336 by hydroclimate and subsurface properties. *Water Resources Research*, 57(10),
1337 e2020WR029469. doi: 10.1029/2020WR029469
- 1338 Erisman, J. W., van Grinsven, H., Grizzetti, B., Bouraoui, F., Powlson, D., Sutton, M. A.,
1339 ... Reis, S. (2011). The European nitrogen problem in a global perspective. In
1340 M. A. Sutton et al. (Eds.), *The european nitrogen assessment: Sources, effects and
1341 policy perspectives* (p. 9—31). Cambridge, UK: Cambridge University Press. doi:
1342 10.1017/CBO9780511976988.005
- 1343 Eschenbach, W., Budziak, D., Elbracht, J., Höper, H., Krienen, L., Kunkel, R., ... Wend-
1344 land, F. (2018). Möglichkeiten und Grenzen der Validierung flächenhaft modellierter
1345 Nitrateinträge ins Grundwasser mit der N₂/Ar-Methode. *Grundwasser*, 23, 125—139.
1346 doi: 10.1007/s00767-018-0391-6
- 1347 European Commission. (2020). *Tenth report on the implementation status and programmes
1348 for implementation (as required by Article 17 of Council Directive 91/271/EEC, con-
1349 cerning urban waste water treatment)* (No. COM/2020/492 final). Brussels, Belgium.
1350 Retrieved from [https://eur-lex.europa.eu/legal-content/EN/TXT/?uri=CELEX:
1351 52020DC0492](https://eur-lex.europa.eu/legal-content/EN/TXT/?uri=CELEX:52020DC0492) (last access: 07 November 2021)
- 1352 Eurostat. (2016). *Population connected to wastewater collection and treatment systems by
1353 nuts 2 regions (env_wwcon_r2) - 11.04.2016 update*. European Commission [data set].

- 1354 Retrieved from https://db.nomics.world/Eurostat/env_wwcon_r2 (last access: 07
1355 November 2021)
- 1356 Eurostat. (2021). *Population connected to wastewater treatment plants (env_ww_con) - 08-*
1357 *02-2021 update*. European Commission [data set]. Retrieved from [http://appsso](http://appsso.eurostat.ec.europa.eu/nui/show.do?lang=en&dataset=env_ww_con)
1358 [.eurostat.ec.europa.eu/nui/show.do?lang=en&dataset=env_ww_con](http://appsso.eurostat.ec.europa.eu/nui/show.do?lang=en&dataset=env_ww_con) (last ac-
1359 cess: 07 November 2021)
- 1360 Eyring, V., Bony, S., Meehl, G. A., Senior, C. A., Stevens, B., Stouffer, R. J., & Taylor,
1361 K. E. (2016). Overview of the Coupled Model Intercomparison Project Phase 6
1362 (CMIP6) experimental design and organization. *Geoscientific Model Development*,
1363 *9*(5), 1937–1958. doi: 10.5194/gmd-9-1937-2016
- 1364 FAO. (1951). *The state of food and agriculture 1951 - Review and overlook*. Rome, Italy:
1365 Food and Agriculture Organization of the United Nations (FAO). Retrieved from
1366 <https://www.fao.org/publications/sofa/en/> (last access: 07 November 2021)
- 1367 FAO. (2021a). *Food balances (old methodology and population) - 12.12.2017 update*. Rome,
1368 Italy: Food and Agriculture Organization of the United Nations (FAO) [data set]. Re-
1369 trieved from <http://www.fao.org/faostat/en/#data/FBSH> (last access: 07 Novem-
1370 ber 2021)
- 1371 FAO. (2021b). *New food balances - 14.04.2021 update*. Rome, Italy: Food and Agriculture
1372 Organization of the United Nations (FAO) [data set]. Retrieved from [http://www](http://www.fao.org/faostat/en/#data/FBS)
1373 [.fao.org/faostat/en/#data/FBS](http://www.fao.org/faostat/en/#data/FBS) (last access: 07 November 2021)
- 1374 FAO and SIK. (2011). *Global food losses and food waste - Extent, causes and preven-*
1375 *tion, Study conducted for the International Congress SAVE FOOD! at Interpack2011*
1376 *Düsseldorf, Germany*. Rome, Italy: Food and Agriculture Organization of the United
1377 Nations (FAO).
- 1378 Farzadfar, S., Knight, J. D., & Congreves, K. A. (2021). Soil organic nitrogen: an overlooked
1379 but potentially significant contribution to crop nutrition. *Plant and Soil*, *462*, 7–23.
1380 doi: 10.1007/s11104-021-04860-w
- 1381 FGG Weser. (2020). *EG-Wasserrahmenrichtlinie, Die wichtigen Fragen der*
1382 *Gewässerbewirtschaftung in der Flussgebietseinheit Weser*. Hildesheim, Germany.
1383 Retrieved from [https://www.fgg-weser.de/oeffentlichkeitsbeteiligung/](https://www.fgg-weser.de/oeffentlichkeitsbeteiligung/veroeffentlichungen/eg-wrrl)
1384 [veroeffentlichungen/eg-wrrl](https://www.fgg-weser.de/oeffentlichkeitsbeteiligung/veroeffentlichungen/eg-wrrl) (last access: 01 March 2021)
- 1385 FGG Weser. (2021). *Weser-Datenbank*. Hildesheim, Germany: Flussgebietsgemein-
1386 schaft (FGG) Weser [data set]. Retrieved from <https://datenbank.fgg-weser.de/>

- 1387 **weserdatenbank** (last access: 07 November 2021)
- 1388 Ford, W. I., Fox, J. F., & Pollock, E. (2017). Reducing equifinality using isotopes in
1389 a process-based stream nitrogen model highlights the flux of algal nitrogen from
1390 agricultural streams. *Water Resources Research*, *53*(8), 6539–6561. doi: 10.1002/
1391 2017WR020607
- 1392 Franko, U., Oelschlägel, B., & Schenk, S. (1995). Simulation of temperature-, water- and
1393 nitrogen dynamics using the model CANDY. *Ecological Modelling*, *81*(1), 213–222.
1394 doi: 10.1016/0304-3800(94)00172-E
- 1395 Global Runoff Data Centre. (2021). *Runoff data*. Koblenz, Germany: Bundesanstalt für
1396 Gewässerkunde [data set]. Retrieved from <http://www.bafg.de/GRDC> (last access:
1397 10 February 2021)
- 1398 Grimvall, A., Stålnacke, P., & Tonderski, A. (2000). Time scales of nutrient losses from
1399 land to sea — A European perspective. *Ecological Engineering*, *14*(4), 363–371. doi:
1400 10.1016/S0925-8574(99)00061-0
- 1401 Grizzetti, B., Bouraoui, F., & De Marsily, G. (2008). Assessing nitrogen pressures on
1402 european surface water. *Global Biogeochemical Cycles*, *22*(4), GB4023. doi: 10.1029/
1403 2007GB003085
- 1404 Gupta, H. V., Kling, H., Yilmaz, K. K., & Martinez, G. F. (2009). Decomposition of
1405 the mean squared error and NSE performance criteria: Implications for improving
1406 hydrological modelling. *Journal of Hydrology*, *377*(1), 80–91. doi: 10.1016/j.jhydrol
1407 .2009.08.003
- 1408 Haag, D., & Kaupenjohann, M. (2001). Landscape fate of nitrate fluxes and emissions
1409 in Central Europe: A critical review of concepts, data, and models for transport
1410 and retention. *Agriculture, Ecosystems & Environment*, *86*(1), 1–21. doi: 10.1016/
1411 S0167-8809(00)00266-8
- 1412 Hanel, M., Rakovec, O., Markonis, Y., Máca, P., Samaniego, L., Kyselý, J., & Kumar,
1413 R. (2018). Revisiting the recent european droughts from a long-term perspective.
1414 *Scientific Reports*, *8*, 9499. doi: 10.1038/s41598-018-27464-4
- 1415 Hansen, S., Jensen, H. E., Nielsen, N. E., & Svendsen, H. (1991). Simulation of nitrogen
1416 dynamics and biomass production in winter wheat using the Danish simulation model
1417 DAISY. *Fertilizer Research*, *27*, 245–259. doi: 10.1007/BF01051131
- 1418 Hartmann, A., Barberá, J. A., & Andreo, B. (2017). On the value of water quality data
1419 and informative flow states in karst modelling. *Hydrology and Earth System Sciences*,

- 1420 21(12), 5971–5985. doi: 10.5194/hess-21-5971-2017
- 1421 Häußermann, U., Klement, L., Breuer, L., Ullrich, A., Wechsung, G., & Bach, M. (2020).
1422 Nitrogen soil surface budgets for districts in Germany 1995 to 2017. *Environmental*
1423 *Sciences Europe*, 32(4), 109. doi: 10.1186/s12302-020-00382-x
- 1424 Heidecke, C., Hirt, U., Kreins, P., Kuhr, P., Kunkel, R., Mahnkopf, J., ... Wendland,
1425 F. T. N. R. . (2015). *Endbericht zum Forschungsprojekt "Entwicklung eines In-*
1426 *strumentes für ein flussgebietsweites Nährstoffmanagement in der Flussgebietsein-*
1427 *heit Weser" - AGRUM+ Weser*. Braunschweig, Germany: Johann Heinrich von
1428 Thünen-Institut. Retrieved from [https://www.thuenen.de/media/publikationen/](https://www.thuenen.de/media/publikationen/thuenen-report/Thuenen-Report_21.pdf)
1429 [thuenen-report/Thuenen-Report_21.pdf](https://www.thuenen.de/media/publikationen/thuenen-report/Thuenen-Report_21.pdf) (last access: 07 November 2021)
- 1430 Hirsch, R. M., Archfield, S. A., & De Cicco, L. A. (2015). A bootstrap method for estimating
1431 uncertainty of water quality trends. *Environmental Modelling & Software*, 73, 148-166.
1432 doi: 10.1016/j.envsoft.2015.07.017
- 1433 Hirsch, R. M., Moyer, D. L., & Archfield, S. A. (2010). Weighted Regressions on Time,
1434 Discharge, and Season (WRTDS), with an application to Chesapeake Bay River inputs.
1435 *Journal of the American Water Resources Association*, 46(5), 857–880. doi: 10.1111/
1436 [j.1752-1688.2010.00482.x](https://doi.org/10.1111/j.1752-1688.2010.00482.x)
- 1437 Hirt, U., Kreins, P., Kuhn, U., Mahnkopf, J., Venohr, M., & Wendland, F. (2012). Man-
1438 agement options to reduce future nitrogen emissions into rivers: A case study of the
1439 Weser river basin, Germany. *Agricultural Water Management*, 115, 118–131. doi:
1440 10.1016/j.agwat.2012.08.005
- 1441 Holland, E. A., Dentener, F. J., Braswell, B. H., & Sulzman, J. M. (1999). Contemporary
1442 and pre-industrial global reactive nitrogen budgets. *Biogeochemistry*, 46, 7–43. doi:
1443 10.1007/BF01007572
- 1444 Hong, B., Swaney, D. P., Mörth, C.-M., Smedberg, E., Eriksson Hägg, H., Humborg, C.,
1445 ... Bouraoui, F. (2012). Evaluating regional variation of net anthropogenic nitrogen
1446 and phosphorus inputs (NANI/NAPI), major drivers, nutrient retention pattern and
1447 management implications in the multinational areas of Baltic Sea basin. *Ecological*
1448 *Modelling*, 227, 117–135. doi: 10.1016/j.ecolmodel.2011.12.002
- 1449 Howarth, R. W., Billen, G., Swaney, D., Townsend, A., Jaworski, N., Lajtha, K., ... Zhao-
1450 Liang, Z. (1996). Regional nitrogen budgets and riverine N & P fluxes for the drainages
1451 to the North Atlantic Ocean: Natural and human influences. *Biogeochemistry*, 35,
1452 75–139. doi: 10.1007/BF02179825

- 1453 Husic, A., Fox, J., Adams, E., Ford, W., Agouridis, C., Currens, J., & Backus, J. (2019).
1454 Nitrate Pathways, Processes, and Timing in an Agricultural Karst System: Devel-
1455 opment and Application of a Numerical Model. *Water Resources Research*, *55*(3),
1456 2079–2103. doi: 10.1029/2018WR023703
- 1457 Ilampooranan, I., Van Meter, K. J., & Basu, N. B. (2019). A Race Against Time: Modeling
1458 Time Lags in Watershed Response. *Water Resources Research*, *55*(5), 3941–3959. doi:
1459 10.1029/2018WR023815
- 1460 Jenkinson, D. S. (1991). The Rothamsted long-term experiments: Are they still of use?
1461 *Agronomy Journal*, *83*(1), 2–10. doi: 10.2134/agronj1991.00021962008300010008x
- 1462 Kaandorp, V. P., Broers, H. P., van der Velde, Y., Rozemeijer, J., & de Louw, P. G. B.
1463 (2021). Time lags of nitrate, chloride, and tritium in streams assessed by dynamic
1464 groundwater flow tracking in a lowland landscape. *Hydrology and Earth System Sci-*
1465 *ences*, *25*(6), 3691–3711. doi: 10.5194/hess-25-3691-2021
- 1466 Kaplan, J. O., & Krumhardt, K. M. (2018). *The KK09 Anthropogenic Land Cover Change*
1467 *Scenarios for Europe and neighboring countries*. PANGAEA [data set]. doi: 10.1594/
1468 PANGAEA.893758
- 1469 Klein Goldewijk, K., Beusen, A., Doelman, J., & Stehfest, E. (2017). Anthropogenic land use
1470 estimates for the Holocene – HYDE 3.2. *Earth System Science Data*, *9*(2), 927–953.
1471 doi: 10.5194/essd-9-927-2017
- 1472 Klein Goldewijk, K., Beusen, A., van Dreht, G., & de Vos, M. (2011). The HYDE 3.1
1473 spatially explicit database of human-induced global land-use change over the past
1474 12,000 years. *Global Ecology and Biogeography*, *20*(1), 73–86. doi: 10.1111/j.1466
1475 -8238.2010.00587.x
- 1476 Knoben, W. J. M., Freer, J. E., & Woods, R. A. (2019). Technical note: Inherent benchmark
1477 or not? Comparing Nash–Sutcliffe and Kling–Gupta efficiency scores. *Hydrology and*
1478 *Earth System Sciences*, *23*(10), 4323–4331. doi: 10.5194/hess-23-4323-2019
- 1479 Knoll, L., Breuer, L., & Bach, M. (2020). Nation-wide estimation of groundwater redox con-
1480 ditions and nitrate concentrations through machine learning. *Environmental Research*
1481 *Letters*, *15*(6), 064004. doi: 10.1088/1748-9326/ab7d5c
- 1482 Koeniger, P., Schwientek, M., Uhlenbrook, S., Leibundgut, C., & Krause, W. J. (2008).
1483 Tritium balance in macro-scale river basins analysed through distributed hydrological
1484 modelling. *Hydrological Processes*, *22*(5), 567–576. doi: 10.1002/hyp.6634
- 1485 Kolmogorov, A. (1933). Sulla determinazione empirica di una legge di distribuzione. *Gior-*

- 1486 *nale dell'Istituto Italiano degli Attuari*, 4, 83–61.
- 1487 Kreins, P., Behrendt, H., Gömann, H., Heidecke, C., Hirt, U., Kunkel, R.,
 1488 ... Wendland, F. (2010). *Analyse von Agrar- und Umweltmaßnahmen im Bereich des landwirtschaftlichen Gewässerschutzes vor dem Hintergrund*
 1489 *der EG-Wasserrahmenrichtlinie in der Flussgebietseinheit Weser (special issue*
 1490 *336)*. Braunschweig, Germany: Johann Heinrich von Thünen-Institut. Re-
 1491 trieved from [https://www.thuenen.de/media/publikationen/landbauforschung-](https://www.thuenen.de/media/publikationen/landbauforschung-sonderhefte/lbf_sh336.pdf)
 1492 [sonderhefte/lbf_sh336.pdf](https://www.thuenen.de/media/publikationen/landbauforschung-sonderhefte/lbf_sh336.pdf) (last access: 07 November 2021)
- 1494 Kumar, R., Samaniego, L., & Attinger, S. (2013). Implications of distributed hydrologic
 1495 model parameterization on water fluxes at multiple scales and locations. *Water Re-*
 1496 *sources Research*, 49(1), 360–379. doi: 10.1029/2012WR012195
- 1497 Lamarque, J.-F., Emmons, L. K., Hess, P. G., Kinnison, D. E., Tilmes, S., Vitt, F., ... Tyn-
 1498 dall, G. K. (2012). CAM-chem: description and evaluation of interactive atmospheric
 1499 chemistry in the Community Earth System Model. *Geoscientific Model Development*,
 1500 5(2), 369–411. doi: 10.5194/gmd-5-369-2012
- 1501 Lee, M., Shevliakova, E., Malyshev, S., Milly, P. C. D., & Jaffé, P. R. (2016). Climate
 1502 variability and extremes, interacting with nitrogen storage, amplify eutrophication
 1503 risk. *Geophysical Research Letters*, 43(14), 7520–7528. doi: 10.1002/2016GL069254
- 1504 Lewis, D. B., & Kaye, J. P. (2012). Inorganic nitrogen immobilization in live and sterile
 1505 soil of old-growth conifer and hardwood forests: implications for ecosystem nitrogen
 1506 retention. *Biogeochemistry*, 111(1), 169–186. doi: 10.1007/s10533-011-9627-6
- 1507 Liu, J., Van Meter, K. J., McLeod, M. M., & Basu, N. B. (2021). Checkered landscapes:
 1508 hydrologic and biogeochemical nitrogen legacies along the river continuum. *Environ-*
 1509 *mental Research Letters*, 16(11), 115006. doi: 10.1088/1748-9326/ac243c
- 1510 Liu, X., Hu, G., He, H., Liang, C., Zhang, W., Bai, Z., ... Zhang, X. (2016). Linking
 1511 microbial immobilization of fertilizer nitrogen to in situ turnover of soil microbial
 1512 residues in an agro-ecosystem. *Agriculture, Ecosystems & Environment*, 229, 40–47.
 1513 doi: 10.1016/j.agee.2016.05.019
- 1514 Lu, C., & Tian, H. (2017). Global nitrogen and phosphorus fertilizer use for agriculture
 1515 production in the past half century: shifted hot spots and nutrient imbalance. *Earth*
 1516 *System Science Data*, 9(1), 181–192. doi: 10.5194/essd-9-181-2017
- 1517 Macdonald, A. J., Powlson, D. S., Poulton, P. R., & Jenkinson, D. S. (1989). Unused
 1518 fertiliser nitrogen in arable soils - Its contribution to nitrate leaching. *Journal of the*

- 1519 *Science of Food and Agriculture*, 46(4), 407–419. doi: 10.1002/jsfa.2740460404
- 1520 MacDonald, G., Levison, J., & Parker, B. (2017). On Methods for In-Well Nitrate Moni-
1521 toring Using Optical Sensors. *Groundwater Monitoring & Remediation*, 37(4), 60–70.
1522 doi: 10.1111/gwmr.12248
- 1523 Mariotti, F., Tomé, D., & Mirand, P. P. (2008). Converting nitrogen into protein—beyond
1524 6.25 and Jones’ factors. *Critical Reviews in Food Science and Nutrition*, 48(2), 177–
1525 184. doi: 10.1080/10408390701279749
- 1526 Martinez, G. F., & Gupta, H. V. (2010). Toward improved identification of hydrological
1527 models: A diagnostic evaluation of the “abcd” monthly water balance model for the
1528 conterminous United States. *Water Resources Research*, 46(8), W08507. doi: 10.1029/
1529 2009WR008294
- 1530 Morée, A. L., Beusen, A. H. W., Bouwman, A. F., & Willems, W. J. (2013). Exploring
1531 global nitrogen and phosphorus flows in urban wastes during the twentieth century.
1532 *Global Biogeochemical Cycles*, 27(3), 836–846. doi: 10.1002/gbc.20072
- 1533 Moriiasi, D. N., Gitau, M. W., Pai, N., & Daggupati, P. (2015). Hydrologic and water
1534 quality models: Performance measures and evaluation criteria. *Transactions of the*
1535 *ASABE*, 58(6), 1763–1785. doi: 10.13031/trans.58.10715
- 1536 Moriiasi, D. N., Zeckoski, R. W., Arnold, J. G., Baffaut, C., Malone, R. W., Daggupati,
1537 P., ... Douglas-Mankin, K. R. (2015). Hydrologic and Water Quality Models: Key
1538 Calibration and Validation Topics. *Transactions of the ASABE*, 58(6), 1609–1618.
1539 doi: 10.13031/trans.58.11075
- 1540 Morier, I., Schleppei, P., Siegwolf, R., Knicker, H., & Guenat, C. (2008). 15N immobilization
1541 in forest soil: a sterilization experiment coupled with 15CPMAS NMR spectroscopy.
1542 *European Journal of Soil Science*, 59(3), 467–475. doi: 10.1111/j.1365-2389.2007
1543 .00998.x
- 1544 Mulholland, P. J., Helton, A. M., Poole, G. C., Hall, R. O., Hamilton, S. K., Peterson, B. J.,
1545 ... Thomas, S. M. (2008). Stream denitrification across biomes and its response to an-
1546 thropogenic nitrate loading. *Nature*, 452(7184), 202–205. doi: 10.1038/nature06686
- 1547 Myhre, D., G., Shindell, F.-M. B., Collins, W., Fuglestedt, J., Huang, J., Koch, D., ...
1548 Zhang, H. (2013). Chapter 8. Anthropogenic and Natural Radiative Forcing. In
1549 T. F. Stocker et al. (Eds.), *Climate Change 2013: The physical science basis. Working*
1550 *Group I contribution to the fifth assessment report of the Intergovernmental Panel on*
1551 *Climate Change* (pp. 659–740). New York, USA: Cambridge University Press.

- 1552 Näsholm, T., Kielland, K., & Ganeteg, U. (2009). Uptake of organic nitrogen by plants.
1553 *New Phytologist*, *182*(1), 31–48. doi: 10.1111/j.1469-8137.2008.02751.x
- 1554 Nguyen, T. V., Kumar, R., Lutz, S. R., Musolff, A., Yang, J., & Fleckenstein, J. H.
1555 (2021). Modeling Nitrate Export From a Mesoscale Catchment Using StorAge Se-
1556 lection Functions. *Water Resources Research*, *57*(2), e2020WR028490. doi: 10.1029/
1557 2020WR028490
- 1558 NLWKN. (2019). *Grundwasserbericht Niedersachsen: Kurzbericht 2019: Grund-*
1559 *wasserstand sowie Güteparameter Nitrat und Arzneimittel im Grundwasser (Band*
1560 *38)*. Hildesheim/Norden, Germany: Niedersächsischer Landesbetrieb für Wasser-
1561 wirtschaft, Küsten- und Naturschutz (NLWKN). Retrieved from [https://](https://www.nlwkn.niedersachsen.de/startseite/wasserwirtschaft/grundwasser/veroeffentlichungen/publikationsreihe-grundwasser/veroeffentlichungen-zum-thema-grundwassertrinkwasser-zum-downloaden-198537.html)
1562 [www.nlwkn.niedersachsen.de/startseite/wasserwirtschaft/grundwasser/](https://www.nlwkn.niedersachsen.de/startseite/wasserwirtschaft/grundwasser/veroeffentlichungen/publikationsreihe-grundwasser/veroeffentlichungen-zum-thema-grundwassertrinkwasser-zum-downloaden-198537.html)
1563 [veroeffentlichungen](https://www.nlwkn.niedersachsen.de/startseite/wasserwirtschaft/grundwasser/veroeffentlichungen/publikationsreihe-grundwasser/veroeffentlichungen-zum-thema-grundwassertrinkwasser-zum-downloaden-198537.html)
1564 [-zum-thema-grundwassertrinkwasser-zum-downloaden-198537.html](https://www.nlwkn.niedersachsen.de/startseite/wasserwirtschaft/grundwasser/veroeffentlichungen/publikationsreihe-grundwasser/veroeffentlichungen-zum-thema-grundwassertrinkwasser-zum-downloaden-198537.html) (last
1565 access: 07 October 2021)
- 1566 NLWKN. (2022). *Landesweite Datenbank für wasserwirtschaftliche Daten*. Norden, Ger-
1567 many: Niedersächsische Landesbetrieb für Wasserwirtschaft, Küsten- und Naturschutz
1568 (NLWKN) [data set]. Retrieved from [http://www.wasserdaten.niedersachsen.de/](http://www.wasserdaten.niedersachsen.de/cadanza/)
1569 [cadanza/](http://www.wasserdaten.niedersachsen.de/cadanza/) (last access: 28 January 2022)
- 1570 OGeV. (2016). *Oberflächengewässerverordnung vom 20. Juni 2016 (BGBl. I S. 1373),*
1571 *die zuletzt durch Artikel 2 Absatz 4 des Gesetzes vom 9. Dezember 2020 (BGBl. I S.*
1572 *2873) geändert worden ist*. Retrieved from [https://www.gesetze-im-internet.de/](https://www.gesetze-im-internet.de/ogewv_2016/index.html)
1573 [ogewv_2016/index.html](https://www.gesetze-im-internet.de/ogewv_2016/index.html) (last access: 07 November 2021)
- 1574 Peters-Lidard, C. D., Clark, M., Samaniego, L., Verhoest, N. E. C., van Emmerik, T.,
1575 Uijlenhoet, R., . . . Woods, R. (2017). Scaling, similarity, and the fourth paradigm for
1576 hydrology. *Hydrology and Earth System Sciences*, *21*(7), 3701–3713. doi: 10.5194/
1577 hess-21-3701-2017
- 1578 Pianosi, F., Beven, K., Freer, J., Hall, J. W., Rougier, J., Stephenson, D. B., & Wagener,
1579 T. (2016). Sensitivity analysis of environmental models: A systematic review with
1580 practical workflow. *Environmental Modelling & Software*, *79*, 214–232. doi: 10.1016/
1581 j.envsoft.2016.02.008
- 1582 Pianosi, F., Sarrazin, F., & Wagener, T. (2015). A Matlab toolbox for Global Sensitivity
1583 Analysis. *Environmental Modelling & Software*, *70*, 80–85. doi: 10.1016/j.envsoft
1584 .2015.04.009

- 1585 Pianosi, F., & Wagener, T. (2015). A simple and efficient method for global sensitivity anal-
1586 ysis based on cumulative distribution functions. *Environmental Modelling & Software*,
1587 *67*, 1–11. doi: 10.1016/j.envsoft.2015.01.004
- 1588 Pianosi, F., & Wagener, T. (2018). Distribution-based sensitivity analysis from a generic
1589 input-output sample. *Environmental Modelling & Software*, *108*, 197–207. doi: 10
1590 .1016/j.envsoft.2018.07.019
- 1591 Poisvert, C., Curie, F., & Moatar, F. (2017). Annual agricultural N surplus in France over
1592 a 70-year period. *Nutrient Cycling in Agroecosystems*, *107*(9), 63–78. doi: 10.1007/
1593 s10705-016-9814-x
- 1594 Portmann, R. W., Daniel, J. S., & Ravishankara, A. R. (2012). Nitrate attenuation in
1595 groundwater: A review of biogeochemical controlling processes. *Philosophical transac-*
1596 *tions of the Royal Society of London. Series B, Biological sciences*, *367*(1593), 1256—
1597 1264. doi: 10.1098/rstb.2011.0377
- 1598 Puckett, L. J., Tesoriero, A. J., & Dubrovsky, N. M. (2011). Nitrogen contamination of
1599 surficial aquifers — A growing legacy. *Environmental Science & Technology*, *45*(3),
1600 839–844. doi: 10.1021/es1038358
- 1601 Queloz, P., Carraro, L., Benettin, P., Botter, G., Rinaldo, A., & Bertuzzo, E. (2015).
1602 Transport of fluorobenzoate tracers in a vegetated hydrologic control volume: 2. The-
1603oretical inferences and modeling. *Water Resources Research*, *51*(4), 2793–2806. doi:
1604 10.1002/2014WR016508
- 1605 Rakovec, O., Kumar, R., Mai, J., Cuntz, M., Thober, S., Zink, M., . . . Samaniego, L. (2016).
1606 Multiscale and multivariate evaluation of water fluxes and states over European river
1607 basins. *Journal of Hydrometeorology*, *17*(1), 287–307. doi: 10.1175/JHM-D-15-0054.1
- 1608 Rankinen, K., Karvonen, T., & Butterfield, D. (2006). An application of the GLUE method-
1609 ology for estimating the parameters of the INCA-N model. *Science of The Total*
1610 *Environment*, *365*(1), 123–139. doi: 10.1016/j.scitotenv.2006.02.034
- 1611 Rivett, M. O., Buss, S. R., Morgan, P., Smith, J. W., & Bemment, C. D. (2008). Nitrate
1612 attenuation in groundwater: A review of biogeochemical controlling processes. *Water*
1613 *Research*, *42*(16), 4215–4232. doi: 10.1016/j.watres.2008.07.020
- 1614 Robertson, G. P., & Groffman, P. M. (2015). Chapter 14 - nitrogen transformations. In
1615 E. A. Paul (Ed.), *Soil microbiology, ecology and biochemistry* (fourth ed., pp. 421–446).
1616 Boston, USA: Academic Press. doi: 10.1016/B978-0-12-415955-6.00014-1
- 1617 Rudolph, D. L., Barry, D. A. J., & Goss, M. J. (1998). Contamination in Ontario farmstead

- 1618 domestic wells and its association with agriculture: 2. Results from multilevel mon-
1619 itoring well installations. *Journal of Contaminant Hydrology*, *32*(3), 295–311. doi:
1620 10.1016/S0169-7722(98)00053-9
- 1621 Samaniego, L., Kumar, R., & Attinger, S. (2010). Multiscale parameter regionalization of
1622 a grid-based hydrologic model at the mesoscale. *Water Resources Research*, *46*(5),
1623 W05523. doi: 10.1029/2008WR007327
- 1624 Samaniego, L., Kumar, R., Thober, S., Rakovec, O., Zink, M., Wanders, N., ... Attinger,
1625 S. (2017). Toward seamless hydrologic predictions across spatial scales. *Hydrology and*
1626 *Earth System Sciences*, *21*(9), 4323–4346. doi: 10.5194/hess-21-4323-2017
- 1627 Sarrazin, F., Hartmann, A., Pianosi, F., Rosolem, R., & Wagener, T. (2018). V2Karst
1628 V1.1: a parsimonious large-scale integrated vegetation–recharge model to simulate
1629 the impact of climate and land cover change in karst regions. *Geoscientific Model*
1630 *Development*, *11*(12), 4933–4964. doi: 10.5194/gmd-11-4933-2018
- 1631 Sarrazin, F., Pianosi, F., & Wagener, T. (2016). Global sensitivity analysis of environmental
1632 models: Convergence and validation. *Environmental Modelling & Software*, *79*, 135–
1633 152. doi: 10.1016/j.envsoft.2016.02.005
- 1634 Scavia, D., & Bricker, S. (2006). Coastal eutrophication assessment in the United States.
1635 *Biogeochemistry*, *79*, 187–208. doi: 10.1007/s10533-006-9011-0
- 1636 Sebilo, M., Mayer, B., Nicolardot, B., Pinay, G., & Mariotti, A. (2013). Long-term fate of
1637 nitrate fertilizer in agricultural soils. *Proceedings of the National Academy of Sciences*,
1638 *110*(45), 18185–18189. doi: 10.1073/pnas.1305372110
- 1639 Seeger, H. (1999). The history of German waste water treatment. *European Water Manage-*
1640 *ment*, *2*(5). Retrieved from <http://www.sewerhistory.org>
1641 [www.sewerhistory.org/
articles/whregion/germany/Seeger.pdf](http://www.sewerhistory.org/articles/whregion/germany/Seeger.pdf) (last access: 07 November 2021)
- 1642 Six, J., Conant, R. T., Paul, E. A., & Paustian, K. (2002). Stabilization mechanisms of soil
1643 organic matter: Implications for C-saturation of soils. *Plant and Soil*, *241*, 155–176.
1644 doi: 10.1023/A:1016125726789
- 1645 Smil, V. (1999). Nitrogen in crop production: An account of global flows. *Global Biogeo-*
1646 *chemical Cycles*, *13*(2), 647–662. doi: 10.1029/1999GB900015
- 1647 Smirnov, N. (1939). On the estimation of the discrepancy between empirical curves of distri-
1648 bution for two independent samples. *Bulletin Mathématique de l'Université Moscou*,
1649 *2*, 3–14.
- 1650 Spoelstra, J., Schiff, S. L., Elgood, R. J., Semkin, R. G., & Jeffries, D. S. (2001). Tracing

- 1651 the Sources of Exported Nitrate in the Turkey Lakes Watershed Using 15N/14N and
1652 18O/16O isotopic ratios. *Ecosystems*, 4, 536–544. doi: 10.1007/s10021-001-0027-y
- 1653 Statistisches Bundesamt. (2021). *Online data portal Genesis, Tables 41120-01-02-4-*
1654 *B and 41141-01-01-4-B*. Wiesbaden, Germany: Gemeinsames Neues Statistisches
1655 Informations-System (GENESIS) [data set]. Retrieved from [https://www](https://www.regionalstatistik.de/genesis/online)
1656 [.regionalstatistik.de/genesis/online](https://www.regionalstatistik.de/genesis/online) (last access: 07 November 2021)
- 1657 Stuart, M., Chilton, P., Kinniburgh, D., & Cooper, D. (2007). Screening for long-term
1658 trends in groundwater nitrate monitoring data. *Quarterly Journal of Engineering*
1659 *Geology and Hydrogeology*, 40(4), 361–376. doi: 10.1144/1470-9236/07-040
- 1660 Sültenfuß, J., Roether, W., & Rhein, M. (2009). The bremen mass spectrometric facility
1661 for the measurement of helium isotopes, neon, and tritium in water. *Isotopes in*
1662 *Environmental and Health Studies*, 45(2), 83–95. doi: 10.1080/10256010902871929
- 1663 Sundermann, G., Wäger, N., Cullmann, A., von Hirschhausen, C., & Kemfert, C. (2020).
1664 Nitrate pollution of groundwater long exceeding trigger value: fertilization practices
1665 require more transparency and oversight. *DIW weekly report*, 8+9/2020, 61–72. doi:
1666 10.18723/diw_dwr:2020-8-1
- 1667 Svirejeva-Hopkins, A., Reis, S., Magid, J., Nardoto, G. B., Barles, S., Bouwman, A. F., ...
1668 Sutton, M. A. (2011). Nitrogen flows and fate in urban landscapes. In M. A. Sut-
1669 ton et al. (Eds.), *The European Nitrogen Assessment: Sources, Effects and Pol-*
1670 *icy Perspectives* (p. 249–270). Cambridge, UK: Cambridge University Press. doi:
1671 10.1017/CBO9780511976988.015
- 1672 Tian, H., Yang, J., Lu, C., Xu, R., Canadell, J. G., Jackson, R. B., ... Zhu, Q. (2018). The
1673 global N₂O model intercomparison project. *Bulletin of the American Meteorological*
1674 *Society*, 99(6), 1231–1251. doi: 10.1175/BAMS-D-17-0212.1
- 1675 Tilmes, S., Lamarque, J.-F., Emmons, L. K., Kinnison, D. E., Marsh, D., Garcia, R. R., ...
1676 Blake, N. (2016). Representation of the Community Earth System Model (CESM1)
1677 CAM4-chem within the Chemistry-Climate Model Initiative (CCMI). *Geoscientific*
1678 *Model Development*, 9(5), 1853–1890. doi: 10.5194/gmd-9-1853-2016
- 1679 United Nations. (2017). *The United Nations World Water Development Re-*
1680 *port 2017, Wastewater: the untapped resource*. Paris, France: UNESCO.
1681 Retrieved from [http://www.unesco.org/new/en/natural-sciences/environment/](http://www.unesco.org/new/en/natural-sciences/environment/water/wwap/wwdr/2017-wastewater-the-untapped-resource/)
1682 [water/wwap/wwdr/2017-wastewater-the-untapped-resource/](http://www.unesco.org/new/en/natural-sciences/environment/water/wwap/wwdr/2017-wastewater-the-untapped-resource/) (last access: 07
1683 November 2021)

- 1684 Van Drecht, G., Bouwman, A. F., Harrison, J., & Knoop, J. M. (2009). Global nitrogen and
1685 phosphate in urban wastewater for the period 1970 to 2050. *Global Biogeochemical*
1686 *Cycles*, *23*(4). doi: 10.1029/2009GB003458
- 1687 Van Meter, K. J., & Basu, N. B. (2015). Catchment legacies and time lags: a parsimonious
1688 watershed model to predict the effects of legacy storage on nitrogen export. *PLoS*
1689 *ONE*, *10*, e0125971. doi: 10.1371/journal.pone.0125971
- 1690 Van Meter, K. J., & Basu, N. B. (2017). Time lags in watershed-scale nutrient transport:
1691 an exploration of dominant controls. *Environmental Research Letters*, *12*(8), 084017.
1692 doi: 10.1088/1748-9326/aa7bf4
- 1693 Van Meter, K. J., Basu, N. B., & Van Cappellen, P. (2017). Two centuries of nitrogen
1694 dynamics: Legacy sources and sinks in the Mississippi and Susquehanna River Basins.
1695 *Global Biogeochemical Cycles*, *31*(1), 2–23. doi: 10.1002/2016GB005498
- 1696 Van Meter, K. J., Basu, N. B., Veenstra, J. J., & Burras, C. L. (2016). The nitrogen legacy:
1697 Emerging evidence of nitrogen accumulation in anthropogenic landscapes. *Environ-*
1698 *mental Research Letters*, *11*(3), 035014. doi: 10.1088/1748-9326/11/3/035014
- 1699 Van Meter, K. J., Van Cappellen, P., & Basu, N. B. (2018). Legacy nitrogen may prevent
1700 achievement of water quality goals in the Gulf of Mexico. *Science*, *360*(6387), 427–430.
1701 doi: 10.1126/science.aar4462
- 1702 Van Puijenbroek, P. J. T. M., Beusen, A. H. W., & Bouwman, A. F. (2019). Global nitrogen
1703 and phosphorus in urban waste water based on the shared socio-economic pathways.
1704 *Journal of Environmental Management*, *231*, 446–456. doi: 10.1016/j.jenvman.2018
1705 .10.048
- 1706 Vero, S., Basu, N., Van Meter, K., Richards, K. G., Mellander, P.-E., Healy, M. G., &
1707 Fenton, O. (2018). Review: the environmental status and implications of the nitrate
1708 time lag in Europe and North America. *Hydrogeology Journal*, *26*, 7–22. doi: 10.1007/
1709 s10040-017-1650-9
- 1710 Wade, A., Jackson, B., & Butterfield, D. (2008). Over-parameterised, uncertain ‘mathemati-
- 1711 cal marionettes’ — How can we best use catchment water quality models? An example
1712 of an 80-year catchment-scale nutrient balance. *Science of The Total Environment*,
1713 *400*(1), 52–74. doi: 10.1016/j.scitotenv.2008.04.030
- 1714 Wang, L., Stuart, M. E., Bloomfield, J. P., Butcher, A. S., Goddy, D. C., McKenzie, A. A.,
1715 ... Williams, A. T. (2012). Prediction of the arrival of peak nitrate concentrations at
1716 the water table at the regional scale in Great Britain. *Hydrological Processes*, *26*(2),

- 1717 226–239. doi: 10.1002/hyp.8164
- 1718 Wang, X., Feng, A., Wang, Q., Wu, C., Liu, Z., Ma, Z., & Wei, X. (2014). Spatial
1719 variability of the nutrient balance and related NPSP risk analysis for agro-ecosystems
1720 in China in 2010. *Agriculture, Ecosystems & Environment*, *193*, 42–52. doi: 10.1016/
1721 j.agee.2014.04.027
- 1722 Wendland, F., Behrendt, H., Gömann, H., Hirt, U., Kreins, P., Kuhn, U., . . . Tetzlaff, B.
1723 (2009). Determination of nitrogen reduction levels necessary to reach groundwater
1724 quality targets in large river basins: the Weser basin case study, Germany. *Nutrient
1725 Cycling in Agroecosystems*, *85*, 63–78. doi: 10.1007/s10705-009-9248-9
- 1726 WHO. (2016). *Nitrate and nitrite in drinking-water - Background docu-
1727 ment for development of WHO Guidelines for Drinking-water Quality* (No.
1728 WHO/FWC/WSH/16.52). Geneva , Switzerland: World Health Organization
1729 (WHO) Press. Retrieved from [https://www.who.int/water_sanitation_health/
1730 dwq/chemicals/nitrate-nitrite-background-jan17.pdf](https://www.who.int/water_sanitation_health/dwq/chemicals/nitrate-nitrite-background-jan17.pdf) (last access: 07 Novem-
1731 ber 2021)
- 1732 Worrall, F., Howden, N., & Burt, T. (2015). Evidence for nitrogen accumulation: The
1733 total nitrogen budget of the terrestrial biosphere of a lowland agricultural catchment.
1734 *Biogeochemistry*, *123*, 411–428. doi: 10.1007/s10533-015-0074-7
- 1735 Wriedt, G., & Rode, M. (2006). Modelling nitrate transport and turnover in a lowland
1736 catchment system. *Journal of Hydrology*, *328*(1), 157–176. doi: 10.1016/j.jhydrol
1737 .2005.12.017
- 1738 Yang, S., Büttner, O., Kumar, R., Jäger, C., Jawitz, J. W., Rao, P., & Borchardt, D.
1739 (2019). Spatial patterns of water quality impairments from point source nutrient
1740 loads in Germany’s largest national River Basin (Weser River). *Science of The Total
1741 Environment*, *697*, 134145. doi: 10.1016/j.scitotenv.2019.134145
- 1742 Yang, X., Jomaa, S., Zink, M., Fleckenstein, J. H., Borchardt, D., & Rode, M. (2018).
1743 A new fully distributed model of nitrate transport and removal at catchment scale.
1744 *Water Resources Research*, *54*(8), 5856–5877. doi: 10.1029/2017WR022380
- 1745 Yansheng, C., Fengliang, Z., Zhongyi, Z., Tongbin, Z., & Huayun, X. (2020). Biotic and
1746 abiotic nitrogen immobilization in soil incorporated with crop residue. *Soil and Tillage
1747 Research*, *202*, 104664. doi: 10.1016/j.still.2020.104664
- 1748 Zhang, B., Tian, H., Lu, C., Dangal, S. R. S., Yang, J., & Pan, S. (2017). Global manure
1749 nitrogen production and application in cropland during 1860–2014: a 5 arcmin gridded

- 1750 global dataset for Earth system modeling. *Earth System Science Data*, 9(2), 667–678.
1751 doi: 10.5194/essd-9-667-2017
- 1752 Zhang, X., Zou, T., Lassaletta, L., Mueller, N. D., Tubiello, F. N., Lisk, M. D., . . . David-
1753 son, E. A. (2021). Quantification of global and national nitrogen budgets for crop
1754 production. *Nature Food*, 2, 529–540. doi: 10.1038/s43016-021-00318-5
- 1755 Zink, M., Kumar, R., Cuntz, M., & Samaniego, L. (2017). A high-resolution dataset of
1756 water fluxes and states for germany accounting for parametric uncertainty. *Hydrology
1757 and Earth System Sciences*, 21(3), 1769–1790. doi: 10.5194/hess-21-1769-2017